





RESEARCH PAPER

Bifurcation analysis of an additional food-provided predator-prey system with anti-predator behavior

Manoj Kumar Singh ^{1,*,‡} and Poonam Poonam ^{1,‡}

¹Department of Mathematics and Statistics, Banasthali Vidyapith, Rajasthan-304022, India

*Corresponding Author

‡ s.manojbbau@gmail.com (Manoj Kumar Singh); poonambanasthali91@gmail.com (Poonam)

Abstract

This article analyzes the qualitative behavior of a predator-prey system where the predator receives extra food and the prey engages in anti-predator behavior to defend itself against attacks by the predator. The positivity and the boundedness of solutions to the system have been examined. The biologically well-posed equilibrium points of the proposed system are derived, and an analysis of their local stability is conducted. In specific situations, it is observed that the solutions of the proposed system are significantly dependent on the initial values. The emergence of several bifurcations in the system, including the saddle-node, Bogdanov-Takens, and Hopf-Andronov, is also shown. Through numerical simulation, the rise of a homoclinic loop is shown. The analytic results are verified by numerical simulations and phase portrait sketches.

Keywords: Additional food; anti-predator behavior; stability; bifurcation

AMS 2020 Classification: 37G10; 34C23; 93D20

1 Introduction

The fragile equilibrium of life on Earth relies on ecological systems, the complex webs of interactions between species and their surroundings. These networks extend from local to global levels, including everything from small ecosystems such as oceans, forests, and wetlands to the entire biosphere. Preserving biodiversity, managing natural resources, and reducing the effects of environmental changes all require an understanding of the dynamics of ecological systems. The dynamics between predators and their prey are one of the fundamental ecological phenomena that have a significant impact on biodiversity. The strong intuition to be alive in predators and prey has led to the development of remarkable strategies in these species. For example, predator species do not rely on a single prey species but rather on a varied range of prey species [1], while prey species exhibit anti-predator behavior [2]. In this article, the impacts of these strategies on a predator-prey system are analyzed.

Researchers are aware that predators exhibit a behavioral adaptation whereby they shift their feeding preferences to alternate food sources in response to decreasing densities of their preferred prey [3]. To develop a comprehensive predator-prey model for such species, it is essential to take into account the inclusion of alternative prey species. The inclusion of supplementary food in a predator-prey system may have a substantial impact on the ecological dynamics and overall stability of ecosystems. For instance, the presence of scavenging possibilities or the introduction of non-native prey species can perturb the ecological balance of the whole system [4]. Moreover, the introduction of this surplus food may have a cascading effect on the ecosystem, impacting not just the populations of prey species and competitors but also those at higher trophic levels [5]. Hence, it is essential to comprehend the ramifications of additional food within predator-prey systems to manage ecosystems and advance conservation initiatives effectively.

The empirical study indicates that the provision of supplementary food to predators does not always result in an increase in predation on target species. Sometimes, it may lead to a reduction in the population density of prey species [3]. This phenomenon is often referred to as “apparent competition” [6]. In addition, the predator population may have short-term advantages via an additional food supply. For instance, using supplementary resources may lead to overexploitation, increasing the likelihood of population collapses or fluctuations [7]. This discrepancy between theory and observations prompted a thorough mathematical investigation of predator-prey systems that include provisions to supply additional food.

Srinivasu et al. [8] developed a predation model including two species to examine the effects of supplementary food provided to the predator species. The researchers noted that manipulating additional food, in terms of quality and quantity, can manage and constrain prey numbers and restrict and eradicate predator populations. The aforementioned theoretical results are consistent with the facts documented in a recent literature review [9] that examines the impact of artificial food sprays on conservation biological control. Prasad et al. [10] created and analyzed an additional food-provided predator-prey system with a Beddington-DeAngelis functional response (a way to incorporate mutual interference between predators). They observed the possibility of the coexistence of predator species with a low density of prey species. This phenomenon contrasts with classical predator-prey models, where the coexistence of predators and prey at low population densities is not attainable. The ramifications of providing alternative food sources to predators in a predator-prey paradigm with harvesting have been studied by Sahoo and Poria [11]. Chakraborty and Das [12] conducted an analysis of the variability of a predator-prey system. They specifically investigated the impact of constant prey refuge and alternative food provided to the predator. The global dynamics of a predator-prey system have been investigated by Sen et al. [13], where the predator is subjected to alternative food as well as harvesting at a constant rate. This work offers valuable methodologies for examining the controllability of systems, which have significant relevance in real-world applications. Shome [14] examined the effects of additional food in a predator-prey model incorporating intraspecific competition among prey species and the theta-logistic prey growth rate. They found that when alternative food sources are limited and intraspecific competition is intense, prey species experience extinction. Consequently, the predator species also face extinction, resulting in the collapse of the whole system. In continuation, they observed that the potential occurrence of this collapse may be averted with the provision of a sufficient amount of alternate sustenance to predatory organisms. This finding suggests that including alternative food sources significantly affects regulating the dynamics of the proposed system. Ghosh et al. [15] studied the dynamics of a predator-prey system with prey refuge and additional food for the predator. Singh et al. [16] performed a qualitative inquiry into a predator-prey model, whereby it was assumed that a continual extra food supply is provided to the predator species and the growth of the predator is regulated by the Allee effect.

Several researchers have recently explored the influence of additional food delivered to predators in predator-prey systems that incorporate various real-life phenomena. For instance, Das et al. [17] used a predator-prey model with prey refuge; Thirthar et al. [18] used a predator-prey model with fear effects, prey refuge, and harvesting; Debnath et al. [19] used a predator-prey system with fear effects and anti-predator behavior; Ananth et al. [20] used a predator-prey model involving Holling-type *III* functional response; Das et al. [21] used a predator-prey model with fear effects; and Umaroh and Savitri [22] used a predator-prey model with Holling-type *III* functional response and anti-predator behavior.

Prey species have evolved a variety of strategies to avoid their natural predators. When preys are threatened, they sometimes display a peculiar defensive behavior in which they sacrifice specific body parts. Lizards, for instance, can release their tails to protect themselves from predators. Adult prey kill juvenile predators to reduce the pressure of future predation and increase population density [23–27]. These kinds of prey behaviors are known as anti-predator behaviors. Zanette et al. [28] performed experiments to demonstrate anti-predator behavior's impact on song sparrows' reproductive rates. The results indicated that implementing such efforts led to a significant reduction of 40% in the song sparrow's reproductive output whenever direct predation was effectively mitigated. As a result, the presence of anti-predator behavior among prey species plays a crucial role in maintaining the intricate equilibrium of predator-prey ecosystems.

Several researchers have examined anti-predator behavior in the context of analyzing nonlinear ecological systems [29–31]. Samanta et al. [31] conducted an analysis of a modified Leslie-Gower model using a Beddington-DeAngelis functional response in order to categorize an anti-predator behavior. Tang and Xiao [32] modified a predator-prey system equipped with a non-monotonic functional response by utilizing anti-predator behavior. The saddle-node, the homoclinic, the Hopf bifurcation, and the Bogdanov-Takens bifurcation of co-dimension two were the bifurcations the authors examined as possible system outcomes. Mortoja et al. [33] presented a stage-structure predator-prey model including anti-predator behavior and group defense. The researchers investigated the system's stability and examined the occurrence of the Hopf bifurcation in the suggested system. A dynamical study is carried out by Savitri [2] on a predator-prey model that is endowed with ratio-dependent functional responses and anti-predator behavior. Recently, Prasad et al. [34] explored the influence of anti-predator behavior on predator-prey dynamics where additional food is provided to predators. They observed that several kinds of bifurcations occur, such as saddle-node bifurcation, Hopf bifurcation, homoclinic bifurcation, and a Bogdanov-Takens bifurcation of co-dimension 2. They concluded that successful implementation of biological control might be achieved by taking the anti-predator behavior as a control parameter. This article employed the Holling type IV functional response (Monod-Haldane), often used in models with predator interference, where high prey density leads to reduced predation rates owing to defensive behaviors shown by prey species. The Holling type II functional response, which is more commonly used, is more suitable for modeling predator-prey interactions where there is a limitation on predator efficiency due to handling time and prey saturation. This research examines the effects of supplementary food in the predator-prey system, including Holling type II functional response and anti-predator behavior. It is observed that the anti-predator behavior enhances the dynamical complexities and can be used as a controlling parameter.

2 The basic mathematical model

Srinivasu et al. [8] proposed a bi-dimensional system of equations to represent a predator-prey dynamic, whereby the predator species are provided with a constant supply of supplementary food distributed equally across the environment. If we assume that the prey species exhibits anti-predator behavior, the model takes the following form:

$$\begin{cases} \frac{du}{dt} = r u \left(1 - \frac{u}{K}\right) - \frac{e_1 uv}{1 + e_1 h_1 u + e_2 h_2 A}, \\ \frac{dv}{dt} = \frac{n_1 e_1 uv + n_2 e_2 A v}{1 + e_1 h_1 u + e_2 h_2 A} - mv - nuv, \end{cases} \quad (1)$$

where $u = u(t)$ and $v = v(t)$ represent the prey and predator populations at time t , respectively. To provide an ecologically appropriate interpretation of the proposed model, it is necessary to assume that $u(0) \geq 0$ and $v(0) \geq 0$. The positive parameters $A, r, K, m, h_1(h_2), n_1(n_2)$ and $e_1(e_2)$ are the amount of additional food, the intrinsic growth rate of prey, the carrying capacity of the environment, the predator’s mortality rate, the handling time of the predator per unit quantity of prey (additional food), the nutritional value of the prey (additional food), and the ability of the predator to detect the prey (additional food), respectively. The term nuv represents anti-predator behavior, and the parameter n is the rate of anti-predator behavior of prey for the predator population. Ecologically, it can be interpreted that this form of anti-predator behavior does not directly benefit the prey population but reduces the growth of the predator population, and in this way, it helps the prey population.

Defining $c = \frac{1}{h_1}, b = n_1 c, a = \frac{1}{e_1 h_1}, \eta = \frac{n_2 e_2}{n_1 e_1}, \alpha = \frac{n_1 h_2}{n_2 h_1}$, the system (1) can be expressed as

$$\begin{cases} \frac{du}{dt} = r u \left(1 - \frac{u}{K}\right) - \frac{c uv}{a + \alpha \eta A + u}, \\ \frac{dv}{dt} = \frac{b(u + \eta A)v}{a + \alpha \eta A + u} - mv - nuv. \end{cases} \quad (2)$$

The ecological interpretation of the parameters a, b , and c in the above model aligns with the conventional predator-prey model. The parameter α is inversely proportional to the additional food quality, and ηA refers to the amount of additional food perceptible to the predator relative to the prey.

Employing the transformations $u = ax, v = \frac{ary}{c}, t = \frac{\hat{t}}{r}$ and dropping the hat, system (2) becomes

$$\begin{cases} \frac{dx}{dt} = x \left(1 - \frac{x}{\gamma}\right) - \frac{xy}{1 + \alpha \zeta + x}, \\ \frac{dy}{dt} = \frac{\beta(x + \zeta)y}{1 + \alpha \zeta + x} - \delta y - \theta xy, \end{cases} \quad (3)$$

where $\gamma = \frac{K}{a}, \beta = \frac{b}{r}, \zeta = \frac{\eta A}{a}, \delta = \frac{m}{r}$ and $\theta = \frac{na}{r}$. From an ecological perspective, our focus is only on the dynamics of system (3) inside the first quadrant $\mathbb{R}_0^+ \times \mathbb{R}_0^+ = \{(x, y) \in \mathbb{R}^2 : x \geq 0, y \geq 0\}$.

- Lemma 1** (i) All solutions of the system (3) initiating in the interior of the positive quadrant of the state space are positive for all $t \geq 0$.
(ii) All solutions of the system (3) initiating in the interior of the positive quadrant of the state space are bounded for all $t \geq 0$.

Proof

(i) The two Eqs. of the system (3) yield

$$x(t) = x(0) \exp \left[\int_0^t \left(1 - \frac{x(\tau)}{\gamma} - \frac{v(\tau)}{1 + \alpha \zeta + u(\tau)} \right) d\tau \right],$$

and

$$y(t) = y(0) \exp \left[\int_0^t \left(\frac{\beta(x(\tau) + \zeta)}{1 + \alpha \zeta + x(\tau)} - \delta - \theta x(\tau) \right) d\tau \right],$$

respectively. The conditions $x(0) \geq 0$ and $y(0) \geq 0$ imply $x(t) \geq 0$ and $y(t) \geq 0$, respectively. Therefore, it can be deduced that a solution originating in the positive quadrant of the xy -plane stays positive throughout.

(ii) The first Eq. of the system (3) yields the following result:

$$\frac{dx}{dt} < x \left(1 - \frac{x}{\gamma} \right).$$

It can be inferred that every solution of the system (3) satisfies $x(t) \leq \gamma$ for all $t > 0$.

Define $\Phi(t) = x(t) + \frac{y(t)}{\beta}$. Then

$$\frac{d\Phi}{dt} = x \left(1 - \frac{x}{\gamma} \right) + \frac{\xi y}{1 + \alpha \xi + x} - \frac{(\delta + \theta x)y}{\beta}.$$

For $\lambda > 0$, we have

$$\frac{d\Phi}{dt} + \lambda \Phi(t) = x \left(1 - \frac{x}{\gamma} + \lambda \right) - \left(\frac{\delta - \lambda}{\beta} - \frac{\xi}{1 + \alpha \xi} \right) y,$$

$$\frac{d\Phi}{dt} + \lambda \Phi(t) \leq \frac{\gamma(1 + \lambda)^2}{4} - \left(\frac{\delta - \lambda}{\beta} - \frac{\xi}{1 + \alpha \xi} \right) y.$$

By selecting a suitably small ($\lambda < \delta$), above inequality can be written as

$$\frac{d\Phi}{dt} + \lambda \Phi(t) < \frac{\gamma(1 + \lambda)^2}{4} + \frac{\xi y}{1 + \alpha \xi}.$$

Thus,

$$\frac{d\Phi}{dt} + \lambda \Phi(t) < \mu,$$

where $\mu = \frac{\gamma(1 + \lambda)^2}{4} + \frac{\xi y}{1 + \alpha \xi}$.

Employing Gronwall's inequality, we get

$$0 < \Phi(t) \leq \frac{\mu}{\lambda} \left(1 - e^{-\lambda t} \right) + \Phi(0) e^{-\lambda t}.$$

The above inequality implies, $0 < \Phi(t) \leq \frac{\mu}{\lambda}$, as $t \rightarrow \infty$. Thus, every solution of the system (3) originating in the positive quadrant of the xy -plane is bounded for all future time.

The above lemma ensures that the system (3) is ecologically well-posed.

3 Existence of equilibrium points

The non-negative solutions of the system $\frac{dx}{dt} = 0$, $\frac{dy}{dt} = 0$ are the constant solutions of the system (3) and are called equilibrium points of the system. It is easy to see that the system (3) has a trivial equilibrium point $E_0(0, 0)$, a predator-free equilibrium point $E_\gamma(\gamma, 0)$, and interior equilibrium

points $E^*(x^*, y^*)$. The abscissa x^* is the root of the quadratic equation

$$\theta x^2 + (\delta + \theta(1 + \alpha\zeta) - \beta)x + \delta(1 + \alpha\zeta) - \beta\zeta = 0. \quad (4)$$

The roots of Eq. (4) are $x^* = \frac{\beta - (\delta + \theta(1 + \alpha\zeta)) \mp \sqrt{(\delta + \theta(1 + \alpha\zeta) - \beta)^2 - 4\theta(\delta(1 + \alpha\zeta) - \beta\zeta)}}{2\theta}$. For the sake of clarity, consider $\Delta_1 = \delta(1 + \alpha\zeta) - \beta\zeta$, $\Delta_2 = \beta - (\delta + \theta(1 + \alpha\zeta))$, and $\Delta_3 = 4\theta\Delta_1$.

To find the equilibrium points of the system (3), we consider the following cases:

Case I: $\Delta_1 > 0$ and $\Delta_2 > 0$.

In this case, if $\Delta_2^2 > \Delta_3$ holds, then the system (3) has two interior equilibrium points $E_1^*(x_1^*, y_1^*)$ and $E_2^*(x_2^*, y_2^*)$, where $x_{1,2}^* = \frac{\Delta_2 \mp \sqrt{\Delta_2^2 - \Delta_3}}{2\theta}$ and $y_{1,2}^* = (1 - \frac{x_{1,2}^*}{\gamma})(1 + \alpha\zeta + x_{1,2}^*)$, provided $\gamma > x_{1,2}^*$; if $\Delta_2^2 = \Delta_3$ holds, then the system (3) has a unique interior equilibrium point $E_3^*(x_3^*, y_3^*)$, where $x_3^* = \frac{\Delta_2}{2\theta}$ and $y_3^* = (1 - \frac{x_3^*}{\gamma})(1 + \alpha\zeta + x_3^*)$, provided $\gamma > x_3^*$; if $\Delta_2^2 < \Delta_3$ holds, then the system (3) has no interior equilibrium point.

Case II: $\Delta_1 < 0$.

In this case, the system (3) has a unique interior equilibrium point $E_4^*(x_4^*, y_4^*)$, where $x_4^* = \frac{\Delta_2 + \sqrt{\Delta_2^2 - \Delta_3}}{2\theta}$ and $y_4^* = (1 - \frac{x_4^*}{\gamma})(1 + \alpha\zeta + x_4^*)$, provided $\gamma > x_4^*$.

Case III: $\Delta_1 = 0$.

In this case, if $\Delta_2 > 0$ holds, the system (3) has an interior equilibrium point $E_5^*(x_5^*, y_5^*)$ and a prey-free equilibrium point $E_6^*(x_6^*, y_6^*) = (0, 1 + \alpha\zeta)$, where $x_5^* = \frac{\Delta_2}{\theta}$ and $y_5^* = (1 - \frac{x_5^*}{\gamma})(1 + \alpha\zeta + x_5^*)$, provided $\gamma > x_5^*$; if $\Delta_2 < 0$ holds, the system (3) has no interior equilibrium point, but a unique prey-free equilibrium point $E_6^*(x_6^*, y_6^*) = (0, 1 + \alpha\zeta)$ occurs.

4 Stability analysis

This section performs an analysis to derive the stability conditions around the equilibrium points determined in the previous section using the linearization technique.

Theorem 1 (i) The equilibrium point $E_0 = (0, 0)$ of system (3) is unstable if $\frac{\beta\zeta}{1 + \alpha\zeta} > \delta$ and saddle if $\frac{\beta\zeta}{1 + \alpha\zeta} < \delta$.

(ii) The equilibrium point $E_\gamma = (\gamma, 0)$ of system (3) is saddle if $\frac{\beta(\gamma + \zeta)}{1 + \alpha\zeta + \gamma} > (\delta + \theta\gamma)$ and asymptotically stable if $\frac{\beta(\gamma + \zeta)}{1 + \alpha\zeta + \gamma} < (\delta + \theta\gamma)$.

Proof

(i) At $E_0(0, 0)$, the Jacobian matrix of the system (3) is

$$J_{E_0} = \begin{pmatrix} 1 & 0 \\ 0 & \frac{\beta\zeta}{1 + \alpha\zeta} - \delta \end{pmatrix}.$$

The eigenvalues of the matrix J_{E_0} are $\lambda_1 = 1 > 0$ and $\lambda_2 = \frac{\beta\zeta}{1 + \alpha\zeta} - \delta$. If $\frac{\beta\zeta}{1 + \alpha\zeta} > \delta$ ($\lambda_2 > 0$), the trivial equilibrium point E_0 is unstable. If $\frac{\beta\zeta}{1 + \alpha\zeta} < \delta$ ($\lambda_2 < 0$), the trivial equilibrium point E_0 is saddle.

(ii) At $E_\gamma(\gamma, 0)$, the Jacobian matrix of the system (3) is

$$J_{E_\gamma} = \begin{pmatrix} -1 & -\frac{\gamma}{1+\alpha\zeta+\gamma} \\ 0 & \frac{\beta(\gamma+\zeta)}{1+\alpha\zeta+\gamma} - (\delta + \theta\gamma) \end{pmatrix}.$$

The eigenvalues of the above matrix are $\lambda_1 = -1 < 0$ and $\lambda_2 = \frac{\beta(\gamma+\zeta)}{1+\alpha\zeta+\gamma} - (\delta + \theta\gamma)$. If $\frac{\beta(\gamma+\zeta)}{1+\alpha\zeta+\gamma} > (\delta + \theta\gamma)$ ($\lambda_2 > 0$), the point E_γ is saddle. If $\frac{\beta(\gamma+\zeta)}{1+\alpha\zeta+\gamma} < (\delta + \theta\gamma)$ ($\lambda_2 < 0$), the point E_γ is stable.

Theorem 2 (i) The equilibrium point $E_1^*(x_1^*, y_1^*)$ of system (3), if it exists, is stable if $\gamma < 1 + \alpha\zeta + 2x_1^*$ and unstable if $\gamma > 1 + \alpha\zeta + 2x_1^*$.

(ii) The equilibrium points $E_2^*(x_2^*, y_2^*)$, $E_4^*(x_4^*, y_4^*)$ and $E_5^*(x_5^*, y_5^*)$ of system (3), if they exist, are always saddle.

(iii) The equilibrium point $E_3^*(x_3^*, y_3^*)$ of system (3), if it exists, is a degenerate singularity.

Proof At $E_i^*(x_i^*, y_i^*)$, $i = 1, 2, 3, 4, 5$, the Jacobian matrix of the system (3) is

$$J_{E_i^*} = \begin{pmatrix} x_i^* \left(-\frac{1}{\gamma} + (1 - \frac{x_i^*}{\gamma}) \frac{1}{1+\alpha\zeta+x_i^*}\right) & -\frac{x_i^*}{1+\alpha\zeta+x_i^*} \\ \left((\beta - \delta) - 2\theta x_i^* - \theta(1 + \alpha\zeta)\right) \left(1 - \frac{x_i^*}{\gamma}\right) & 0 \end{pmatrix}.$$

The determinant and trace of the matrix $J_{E_i^*}$ are $\det J_{E_i^*} = \frac{x_i^* y_i^*}{(1+\alpha\zeta+x_i^*)^2} (\Delta_2 - 2\theta x_i^*)$ and $\text{tr } J_{E_i^*} = \frac{x_i^*}{\gamma(1+\alpha\zeta+x_i^*)} (\gamma - (1 + \alpha\zeta + 2x_i^*))$, respectively.

(i) It is easy to show that $\det J_{E_1^*} = \frac{x_1^* y_1^*}{(1+\alpha\zeta+x_1^*)^2} (\sqrt{(\Delta_2^2 - \Delta_3)} > 0$ and $\text{tr } J_{E_1^*} = \frac{x_1^*}{\gamma(1+\alpha\zeta+x_1^*)} (\gamma - (1 + \alpha\zeta + 2x_1^*))$. The Routh-Hurwitz criteria confirm the result.

(ii) A simple calculation may provide $\det J_{E_2^*} = -\frac{x_2^* y_2^*}{(1+\alpha\zeta+x_2^*)^2} (\sqrt{(\Delta_2^2 - \Delta_3)} < 0$, $\det J_{E_4^*} = -\frac{x_4^* y_4^*}{(1+\alpha\zeta+x_4^*)^2} (\sqrt{(\Delta_2^2 - \Delta_3)} < 0$, and $\det J_{E_5^*} = -\frac{x_5^* y_5^* \sqrt{\Delta_2}}{(1+\alpha\zeta+x_5^*)^2} < 0$. Thus, the result follows.

(iii) It is easy to show that $\det J_{E_3^*} = 0$. Thus, the equilibrium point E_3^* is a degenerate singularity.

Theorem 3 The equilibrium point E_3^* of system (3), if exists, then it is

(i) a stable saddle-node if $\gamma < 1 + \alpha\zeta + 2x_3^*$ and an unstable saddle-node if $\gamma > 1 + \alpha\zeta + 2x_3^*$.

(ii) a cusp of codimension 2 if $\gamma = 1 + \alpha\zeta + 2x_3^*$ and $\eta_1 \eta_2 \neq 0$.

Proof

(i) Firstly, we employ the transformations $\check{x} = x - x_3^*$, $\check{y} = y - y_3^*$, the equilibrium point E_3^* shifts to the origin $(0, 0)$. Using Taylor series expansion centered at $(0, 0)$, the system (3) reduces to

$$\begin{cases} \frac{d\check{x}}{dt} = a_{10}\check{x} + a_{01}\check{y} + a_{20}\check{x}^2 + a_{11}\check{x}\check{y} + o(|\check{x}, \check{y}|^3), \\ \frac{d\check{y}}{dt} = b_{10}\check{x} + b_{01}\check{y} + b_{20}\check{x}^2 + b_{11}\check{x}\check{y} + b_{02}\check{y}^2 + o(|\check{x}, \check{y}|^3), \end{cases} \quad (5)$$

where $a_{10} = \frac{x_3^*}{\gamma(1+\alpha\zeta+x_3^*)} (\gamma - (1 + \alpha\zeta + 2x_3^*))$, $a_{01} = -\frac{x_3^*}{1+\alpha\zeta+x_3^*}$, $a_{20} = -\frac{1}{\gamma} + \frac{(1+\alpha\zeta)y_3^*}{(1+\alpha\zeta+x_3^*)^3}$, $a_{11} = -\frac{(1+\alpha\zeta)}{(1+\alpha\zeta+x_3^*)^2}$, $b_{10} = \left(\frac{\beta(1+\alpha\zeta-\zeta)}{(1+\alpha\zeta+x_3^*)^2} - \theta\right) y_3^*$, $b_{01} = 0$, $b_{20} = -\frac{\beta(1+\alpha\zeta-\zeta)y_3^*}{(1+\alpha\zeta+x_3^*)^3}$, $b_{11} = \frac{\beta(1+\alpha\zeta-\zeta)}{(1+\alpha\zeta+x_3^*)^2} - \theta$, $b_{02} = 0$.

It is simple to check if $a_{10} \neq 0$, i.e., $\gamma \neq 1 + \alpha\zeta + 2x_3^*$, then the $\text{tr}(J_{E_3^*}) \neq 0$ but $\det(J_{E_3^*}) = 0$. Thus, the equilibrium point E_3^* is a saddle node. Furthermore, if $\gamma < 1 + \alpha\zeta + 2x_3^*$, i.e., $\text{tr}(J_{E_3^*}) < 0$, the equilibrium point E_3^* is a stable saddle node. If $\gamma > 1 + \alpha\zeta + 2x_3^*$, i.e., $\text{tr}(J_{E_3^*}) > 0$, the equilibrium point E_3^* is an unstable saddle node.

(ii) If $\gamma = 1 + \alpha\zeta + 2x_3^*$, then $\text{tr}(J_{E_3^*}) = 0$ and $\det(J_{E_3^*}) = 0$. By applying the transformation $\tilde{x} = \tilde{x}$, $\tilde{y} = a_{10}\tilde{x} + a_{01}\tilde{y}$, the system (5) reduces to

$$\begin{cases} \frac{d\tilde{x}}{dt} = \tilde{y} + \overline{a_{20}}\tilde{x}^2 + \overline{a_{11}}\tilde{x}\tilde{y} + o(|\tilde{x}, \tilde{y}|^3), \\ \frac{d\tilde{y}}{dt} = \overline{b_{20}}\tilde{x}^2 + \overline{b_{11}}\tilde{x}\tilde{y} + o(|\tilde{x}, \tilde{y}|^3), \end{cases} \quad (6)$$

where $\overline{a_{20}} = a_{20} - \frac{a_{11}a_{10}}{a_{01}}$, $\overline{a_{11}} = \frac{a_{11}}{a_{01}}$, $\overline{b_{20}} = a_{10}a_{20} + a_{01}b_{20} - b_{11}a_{10} - \frac{a_{11}a_{10}^2}{a_{01}}$, $\overline{b_{11}} = \frac{a_{11}a_{10}}{a_{01}} + b_{11}$. By applying the transformations $w_1 = \tilde{x} - \frac{1}{2}\overline{a_{11}}\tilde{x}^2$, $w_2 = \tilde{y} + \overline{a_{20}}\tilde{x}^2$, the system (6) reduces to

$$\begin{cases} \frac{dw_1}{dt} = w_2 + o(|w_1, w_2|^3), \\ \frac{dw_2}{dt} = \eta_1 w_1^2 + \eta_2 w_1 w_2 + o(|w_1, w_2|^3), \end{cases} \quad (7)$$

where $\eta_1 = \overline{b_{20}}$ and $\eta_2 = 2\overline{a_{20}} + \overline{b_{11}}$.

Finally, applying the transformations $z_1 = w_1$, $z_2 = w_2 + o(|w_1, w_2|^3)$, the system (7) reduces to

$$\begin{cases} \frac{dz_1}{dt} = z_2, \\ \frac{dz_2}{dt} = \eta_1 z_1^2 + \eta_2 z_1 z_2 + o(|z_1, z_2|^3). \end{cases}$$

The non-degeneracy condition $\eta_1 \eta_2 = \overline{b_{20}}(2\overline{a_{20}} + \overline{b_{11}}) \neq 0$ for a cusp with co-dimension 2 is satisfied in the $z_1 z_2$. Consequently, the point E_3^* is a cusp of co-dimension 2.

Theorem 4 The equilibrium point $E_6^*(u_6^*, v_6^*)$ of the system (3) is a cusp of co-dimension 2 if $\gamma \neq 1 + \alpha\zeta$.

Proof At $E_6^*(x_6^*, y_6^*)$, the Jacobian matrix of the system (3) is

$$J_{E_6^*} = \begin{pmatrix} 0 & 0 \\ \frac{\beta(1+\alpha\zeta-\zeta)}{1+\alpha\zeta} - \theta(1+\alpha\zeta) & 0 \end{pmatrix}.$$

The determinant and trace of the above matrix are zero. To relocate the equilibrium point E_6^* to the origin, we consider transformations $X = x - x_6^*$, $Y = y - y_6^*$. The Taylor series expansion centered at $(0, 0)$ reduces the system (3) as follows:

$$\begin{cases} \frac{dX}{dt} = \alpha_{20}X^2 + \alpha_{11}XY + o(|X, Y|^3), \\ \frac{dY}{dt} = \beta_{10}X + \beta_{20}X^2 + \beta_{11}XY + o(|X, Y|^3), \end{cases} \quad (8)$$

where $\alpha_{20} = \left(-\frac{1}{\gamma} + \frac{1}{1+\alpha\zeta}\right)$, $\alpha_{11} = -\frac{1}{1+\alpha\zeta}$, $\beta_{10} = \frac{\beta(1+\alpha\zeta-\zeta)}{1+\alpha\zeta} - \theta(1+\alpha\zeta)$, $\beta_{20} = -\frac{\beta(1+\alpha\zeta-\zeta)}{(1+\alpha\zeta)^2}$, $\beta_{11} = \frac{\beta(1+\alpha\zeta-\zeta)}{(1+\alpha\zeta)^2} - \theta$. Introduce a new time variable T by $T = \beta_{10}t$, the system (8) reduced to

$$\begin{cases} \frac{dX}{dT} = \alpha_{20}X^2 + \alpha_{11}XY + o(|X, Y|^3), \\ \frac{dY}{dT} = X + \beta_{20}X^2 + \beta_{11}XY + o(|X, Y|^3), \end{cases} \quad (9)$$

where $\alpha_{20}^- = \frac{\alpha_{20}}{\beta_{10}}$, $\alpha_{11}^- = \frac{\alpha_{11}}{\beta_{10}}$, $\beta_{20}^- = \frac{\beta_{20}}{\beta_{10}}$, $\beta_{11}^- = \frac{\beta_{11}}{\beta_{10}}$.

By applying the transformations $Y_1 = Y - \frac{1}{2}\beta_{11}^- Y^2$, $X_1 = X + \beta_{20}^- X^2$, system (9) reduces to

$$\begin{cases} \frac{dX_1}{dT} = \vartheta_1 X_1^2 + \vartheta_2 X_1 Y_1 + o(|(X_1, Y_1)|^3), \\ \frac{dY_1}{dT} = X_1 + o(|(X_1, Y_1)|^3), \end{cases} \quad (10)$$

where $\vartheta_1 = \alpha_{20}^-$, $\vartheta_2 = \alpha_{11}^-$.

Finally, applying the transformations $Y_2 = Y_1$, $X_2 = X_1 + o(|(X_2, Y_2)|^3)$, the system (10) reduces to

$$\begin{cases} \frac{dX_2}{dT} = \vartheta_1 X_2^2 + \vartheta_2 X_2 Y_2 + o(|(X_2, Y_2)|^3), \\ \frac{dY_2}{dT} = X_2. \end{cases}$$

The non-degeneracy condition $\vartheta_1 \vartheta_2 \neq 0$, i.e., $\frac{1}{1+\alpha\zeta} \left(-\frac{1}{\gamma} + \frac{1}{1+\alpha\zeta} \right) \neq 0$ for cusp of co-dimension 2 can be satisfied in the $X_2 Y_2$ plane, if $\gamma \neq 1 + \alpha\zeta$. As a result, the equilibrium point E_6^* is a cusp of co-dimension 2.

5 Bifurcation analysis

In this section of the article, we are interested in a variety of distinct bifurcations that might take place in the system (3), such as saddle-node, Bogdanov-Takens, and Hopf bifurcations.

Saddle-node bifurcation

In Section 3, the requirements necessary for the existence of two interior equilibrium points $E_1^*(x_1^*, y_1^*)$ and $E_2^*(x_2^*, y_2^*)$ have been achieved that were based on many constraints. The distinguishable features of these equilibrium points persist until $\Delta_1 > 0$, $\Delta_2 > 0$ and $\Delta_2^2 > \Delta_3$; afterward, they have a chance of converging to $E_3^*(x_3^*, y_3^*)$ if $\Delta_1 > 0$, $\Delta_2 > 0$ and $\Delta_2^2 = \Delta_3$ and vanishing if $\Delta_1 > 0$, $\Delta_2 > 0$ and $\Delta_2^2 < \Delta_3$. This kind of annihilation of equilibrium points may be due to the saddle-node bifurcation for interior equilibrium points, which transpires when the bifurcation parameter θ satisfies $\theta = \theta^* = \frac{((\delta+\beta)(1+\alpha\zeta)-2\beta\zeta)-2\sqrt{\Delta_4}}{(1+\alpha\zeta)^2}$, provided $(\delta + \beta)(1 + \alpha\zeta) > 2\beta\zeta$ and $\delta(1 + \alpha\zeta) > \zeta(\delta + \beta)$, where $\Delta_4 = (\delta(1 + \alpha\zeta) - \zeta(\delta + \beta))\beta(1 + \alpha\zeta) + \beta^2\zeta^2$. Here, θ^* is known as the saddle-node bifurcation threshold. Sotomayor’s theorem [38] has been applied to ascertain the occurrence of the bifurcation.

Theorem 5 *System (3) exhibits a saddle-node bifurcation at the equilibrium point $E_3^* = (x_3^*, y_3^*)$ with respect to the parameter θ if $\theta = \theta^* = \frac{((\delta+\beta)(1+\alpha\zeta)-2\beta\zeta)-2\sqrt{\Delta_4}}{(1+\alpha\zeta)^2}$, provided, $(\delta + \beta)(1 + \alpha\zeta) > 2\beta\zeta$ and $\delta(1 + \alpha\zeta) > \zeta(\delta + \beta)$, where $\Delta_4 = (\delta(1 + \alpha\zeta) - \zeta(\delta + \beta))\beta(1 + \alpha\zeta) + \beta^2\zeta^2$.*

Proof The Jacobian matrix for system (3) at interior equilibrium point E_3^* is

$$J_{E_3^*} = \begin{bmatrix} \frac{(\beta-\delta-\theta(1+\alpha\zeta))(\gamma\theta+\delta-\beta)}{\gamma\theta(\beta-\delta+\theta(1+\alpha\zeta))} & \frac{-(\beta-\delta-\theta(1+\alpha\zeta))}{\beta-\delta+\theta(1+\alpha\zeta)} \\ 0 & 0 \end{bmatrix}.$$

The eigenvalues of the above matrix are $\lambda_1 = \frac{(\beta-\delta-\theta(1+\alpha\zeta))(\gamma\theta+\delta-\beta)}{\gamma\theta(\beta-\delta+\theta(1+\alpha\zeta))} \neq 0$ and $\lambda_2 = 0$. Let P and Q be the eigenvectors corresponding to $\lambda_2 = 0$ for the matrices $J_{E_3^*}$ and $J_{E_3^*}^T$, respectively.

A straightforward calculation implies

$$P = \begin{bmatrix} 1 \\ \frac{\gamma\theta + \delta - \beta}{\gamma\theta} \end{bmatrix}, \quad Q = \begin{bmatrix} 0 \\ 1 \end{bmatrix}.$$

Consider

$$\psi(x, y, \theta) = \begin{bmatrix} 1 - \frac{x}{\gamma} - \frac{y}{1 + \alpha\zeta + x} \\ \frac{\beta(x + \zeta)}{1 + \alpha\zeta + x} - \delta - \theta x \end{bmatrix}.$$

One can easily find,

$$\psi_\theta(E_3^*, \theta^*) = \begin{bmatrix} 0 \\ \frac{-(\beta - \delta - \theta(1 + \alpha\zeta))}{2\theta} \end{bmatrix},$$

and

$$D^2\psi(E_3^*, \theta^*)(P, P) = \begin{bmatrix} \frac{-4\theta(2\theta\gamma - (\beta - \delta - \theta(1 + \alpha\zeta)))}{\gamma(\beta - \delta + \theta(1 + \alpha\zeta))^2} + \frac{8\theta(\gamma\theta + \delta - \beta)}{\gamma(\beta - \delta + \theta(1 + \alpha\zeta))} \\ \frac{-16\beta\theta^3(1 + \alpha\zeta - \zeta)}{(\beta - \delta + \theta(1 + \alpha\zeta))^3} \end{bmatrix}.$$

We have

$$Q^T \cdot \psi_\theta(E_3^*, \theta^*) = \frac{-(\beta - \delta - \theta(1 + \alpha\zeta))}{2\theta} \neq 0,$$

and

$$Q^T \cdot D^2\psi(E_3^*, \theta^*)(P, P) = \frac{-16\beta\theta^3(1 + \alpha\zeta - \zeta)}{(\beta - \delta + \theta(1 + \alpha\zeta))^3} \neq 0.$$

Therefore, the transversality conditions necessary for the appearance of the saddle-node bifurcation are satisfied, thereby confirming the presence of a saddle-node bifurcation.

Hopf bifurcation

Theorem 2 concludes that the equilibrium point $E_1^* = (x_1^*, y_1^*)$ is unstable if $1 + \alpha\zeta + 2x_1^* < \gamma$ and stable if $1 + \alpha\zeta + 2x_1^* > \gamma$. It is interesting to investigate the nature of the point E_1^* whenever $\gamma - (1 + \alpha\zeta + 2x_1^*) = 0$.

Theorem 6 Assume that the equilibrium point $E_1^* = (x_1^*, y_1^*)$ exists. For the parametric condition, $\gamma - (1 + \alpha\zeta + 2x_1^*) = 0$, system (3) undergoes a Hopf bifurcation around the equilibrium point E_1^* with respect to the parameter γ .

Proof We have $\det(J_{E_1^*}) > 0$. The parametric condition $\gamma = \gamma^{[hf]} = 1 + \alpha\zeta + 2x_1^*$ implies $\text{tr}(J_{E_1^*}) = 0$. Further, at $\gamma = \gamma^{[hf]} = 1 + \alpha\zeta + 2x_1^*$

$$\frac{d}{d\gamma} \left(\text{tr}(J_{E_1^*}) \right) \Big|_{\gamma=\gamma^{[hf]}} = \frac{x_1^*(1 + \zeta + 2x_1^*)}{\gamma^2(1 + \alpha\zeta + x_1^*)} \neq 0.$$

Thus, the transversality requirement necessary for the appearance of the Hopf bifurcation is satisfied, thereby confirming the presence of a Hopf bifurcation.

The aforementioned theorem is sure enough for the emergence of the limit cycle around the point E_1^* . However, it provides no insight into the stability of the limit cycle. In this continuation, we will proceed with the computation of the first Lyapunov number for the system (3) at the point E_1^* . This calculation will enable us to ascertain the stability of the limit cycle.

To relocate the point E_1^* , to the origin $(0, 0)$, we substitute $x = \bar{x} - x_1^*$ and $y = \bar{y} - y_1^*$. The system (3) reduces to

$$\begin{cases} \frac{d\bar{x}}{dt} = \alpha_{10}\bar{x} + \alpha_{01}\bar{y} + \alpha_{20}\bar{x}^2 + \alpha_{11}\bar{x}\bar{y} + \alpha_{02}\bar{y}^2 + \alpha_{30}\bar{x}^3 + \alpha_{21}\bar{x}^2\bar{y} + \alpha_{12}\bar{x}\bar{y}^2 + \alpha_{03}\bar{y}^3 + g_1(\bar{x}, \bar{y}), \\ \frac{d\bar{y}}{dt} = \beta_{10}\bar{x} + \beta_{01}\bar{y} + \beta_{20}\bar{x}^2 + \beta_{11}\bar{x}\bar{y} + \beta_{02}\bar{y}^2 + \beta_{30}\bar{x}^3 + \beta_{21}\bar{x}^2\bar{y} + \beta_{12}\bar{x}\bar{y}^2 + \beta_{03}\bar{y}^3 + g_2(\bar{x}, \bar{y}), \end{cases} \quad (11)$$

where $\alpha_{10} = x_1^* \left(\frac{-1}{\gamma} + \frac{y_1^*}{(1+\alpha\zeta+x_1^*)^2} \right)$, $\alpha_{01} = \frac{-x_1^*}{1+\alpha\zeta+x_1^*}$, $\alpha_{20} = \left(\frac{-1}{\gamma} + \frac{y_1^*(1+\alpha\zeta)}{(1+\alpha\zeta+x_1^*)^3} \right)$, $\alpha_{11} = \frac{-(1+\alpha\zeta)}{(1+\alpha\zeta+x_1^*)^2}$, $\alpha_{02} = 0$, $\alpha_{30} = \frac{-y_1^*(1+\alpha\zeta)}{(1+\alpha\zeta+x_1^*)^4}$, $\alpha_{21} = \frac{1+\alpha\zeta}{(1+\alpha\zeta+x_1^*)^3}$, $\alpha_{12} = 0$, $\alpha_{03} = 0$, $\beta_{10} = y_1^* \left(\frac{(\beta(1+\alpha\zeta-\zeta))}{(1+\alpha\zeta+x_1^*)^2} - \theta \right)$, $\beta_{01} = 0$, $\beta_{20} = \frac{-y_1^*\beta(1+\alpha\zeta-\zeta)}{1+\alpha\zeta+x_1^*}$, $\beta_{11} = \frac{\beta(1+\alpha\zeta-\zeta)}{(1+\alpha\zeta+x_1^*)^2} - \theta$, $\beta_{02} = 0$, $\beta_{30} = \frac{y_1^*\beta(1+\alpha\zeta-\zeta)}{(1+\alpha\zeta+x_1^*)^4}$, $\beta_{21} = \frac{-\beta(1+\alpha\zeta-\zeta)}{(1+\alpha\zeta+x_1^*)^3}$, $\beta_{12} = 0$, $\beta_{03} = 0$, and $g_1(\bar{x}, \bar{y}) = \sum_{i+j=4}^{\infty} \alpha_{ij}\bar{x}^i\bar{y}^j$, $g_2(\bar{x}, \bar{y}) = \sum_{i+j=4}^{\infty} \beta_{ij}\bar{x}^i\bar{y}^j$.

The first Lyapunov number [38] at the origin is

$$\begin{aligned} \sigma = & \frac{-3\pi}{2\alpha_{01}\Delta^{3/2}} \{ [\alpha_{10}\beta_{10}M_1 + \alpha_{10}\alpha_{01}M_2 + \beta_{10}^2M_3 + 2\alpha_{10}\beta_{10}(\alpha_{20}\alpha_{02} - \beta_{02}^2) \\ & + 2\alpha_{10}\alpha_{01}(\beta_{20}\beta_{02} - \alpha_{20}^2) - \alpha_{01}^2(\beta_{11}\beta_{20} + 2\alpha_{20}\beta_{20}) + (2\alpha_{10}^2 - \alpha_{01}\beta_{10})(\alpha_{11}\alpha_{20} - \beta_{11}\beta_{02})] \\ & - (\alpha_{10}^2 + \alpha_{01}\beta_{10})M_4 \}, \end{aligned} \quad (12)$$

where, $M_1 = \alpha_{02}\beta_{11} + \alpha_{11}\beta_{02} + \alpha_{11}^2$, $M_2 = \alpha_{11}\beta_{02} + \alpha_{20}\beta_{11} + \beta_{11}^2$, $M_3 = 2\alpha_{02}\beta_{02} + \alpha_{11}\alpha_{02}$, $M_4 = \alpha_{12}\beta_{10} - \beta_{21}\alpha_{01} + 2\alpha_{10}(\beta_{12} + \alpha_{21}) + 3(\beta_{03}\beta_{10} - \alpha_{30}\alpha_{01})$, and $\Delta = \frac{x_1^*y_1^*}{(1+\alpha\zeta+x_1^*)^2} \sqrt{\Delta_2^2 - \Delta_3}$. If $\sigma > 0$, then a subcritical Hopf-bifurcation appears around the point E_1^* and the limit cycle will be unstable. If $\sigma < 0$, then a supercritical Hopf-bifurcation appears around the point E_1^* , and the limit cycle will be stable.

Bogdanove-taken bifurcation

In addition to the codimension one bifurcations that have been studied up to this point, it is also conceivable for the system (3) to experience a codimension two bifurcation, such as a Bogdanov-Takens (BT) bifurcation. This bifurcation is expected to take place in the vicinity of the point E_3^* , which is identified as a cusp of co-dimension two under certain parametric constraints.

Theorem 7 Assume that the point E_3^* exists and that it is a cusp of codimension two. If γ and θ are the bifurcation parameters, the system (3) experiences the Bogdanov-Takens bifurcation of codimension 2 in the vicinity of E_3^* .

Proof Here, our objective is to provide analytical expressions for the saddle-node bifurcation curve, Hopf bifurcation curve, and homoclinic bifurcation curve in the vicinity of the Bogdanov-Takens (BT) point. To accomplish our objective, we use the approach defined in the works [36, 37]. Let γ_{BT} and θ_{BT} represent the threshold values of the bifurcation parameters γ and θ that satisfy $\det J_{E_3} = 0$, $\text{tr} J_{E_3} = 0$. Consider a perturbation to the parameters γ and θ in the vicinity of BT

bifurcation values provided by $\gamma = \gamma_{BT} + \lambda_1$ and $\theta = \theta_{BT} + \lambda_2$, respectively, where $\lambda = (\lambda_1, \lambda_2)$ is a parameter vector in the vicinity of $(0, 0)$.

When we substitute these perturbations into system (3), we obtain

$$\begin{cases} \frac{dx}{dt} = x(1 - \frac{x}{\gamma_{BT} + \lambda_1}) - \frac{xy}{1 + \alpha\xi + x} = f_1(x, y, \lambda_1), \\ \frac{dy}{dt} = \frac{\beta(x + \xi)y}{1 + \alpha\xi + x} - \delta y - (\theta_{BT} + \lambda_2)xy = f_2(x, y, \lambda_2). \end{cases} \quad (13)$$

The transformations $U = x - x_3^*$, $V = y - y_3^*$ are taken into consideration to relocate the point E_3^* to the origin $(0, 0)$. After applying Taylor's series expansion centered at $(0, 0)$, the system (13) becomes

$$\begin{cases} \frac{dU}{dt} = \alpha_{00} + \alpha_{10}U + \alpha_{01}V + \alpha_{20}U^2 + \alpha_{11}UV + P_1(U, V), \\ \frac{dV}{dt} = \beta_{00} + \beta_{10}U + \beta_{01}V + \beta_{20}U^2 + \beta_{11}UV + P_2(U, V), \end{cases} \quad (14)$$

where $\alpha_{00} = f_1(U, V, \lambda_1)$, $\alpha_{10} = 1 - \frac{2x_3^*}{\gamma_{BT} + \lambda_1} - \frac{(1 + \alpha\xi)y_3^*}{(1 + \alpha\xi + x_3^*)^2}$, $\alpha_{01} = -\frac{x_3^*}{1 + \alpha\xi + x_3^*}$, $\alpha_{20} = -\frac{1}{\gamma_{BT} + \lambda_1} + \frac{(1 + \alpha\xi)y_3^*}{(1 + \alpha\xi + x_3^*)^3}$, $\alpha_{11} = -\frac{(1 + \alpha\xi)}{(1 + \alpha\xi + x_3^*)^2}$, $\alpha_{02} = 0$, $\beta_{00} = -\lambda_2 x_3^* y_3^*$, $\beta_{10} = \frac{\beta(1 + \alpha\xi - \xi)y_3^*}{(1 + \alpha\xi + x_3^*)^2} - (\theta_{BT} + \lambda_2)y_3^*$,

$\beta_{01} = -\lambda_2 x_3^*$, $\beta_{11} = \frac{\beta(1 + \alpha\xi - \xi)}{(1 + \alpha\xi + x_3^*)^2} - (\theta_{BT} + \lambda_2)$, $\beta_{02} = 0$, and P_1, P_2 is power series in (U, V) with powers $x^i y^j$ satisfying $i + j \geq 3$, and the coefficients smoothly depend upon λ_1 and λ_2 .

After using the affine transformation $U_1 = U$, $U_2 = \alpha_{10}U + \alpha_{01}V$, the system (14) simplifies to

$$\begin{cases} \frac{dU_1}{dt} = \xi_{00} + U_2 + \xi_{20}U_1^2 + \xi_{11}U_1U_2 + \tilde{P}_1(U_1, U_2), \\ \frac{dU_2}{dt} = \mu_{00} + \mu_{10}U_1 + \mu_{01}U_2 + \mu_{20}U_1^2 + \mu_{11}U_1U_2 + \tilde{P}_2(U_1, U_2), \end{cases} \quad (15)$$

where $\xi_{00} = \alpha_{00}$, $\xi_{20} = \alpha_{20} - \frac{\alpha_{11}\alpha_{10}}{\alpha_{01}}$, $\xi_{11} = \frac{\alpha_{11}}{\alpha_{01}}$, $\mu_{00} = \alpha_{00}\alpha_{10} + \beta_{00}\alpha_{01}$, $\mu_{10} = \alpha_{10}\beta_{10} - \beta_{01}\alpha_{10}$, $\mu_{01} = \alpha_{10} + \beta_{01}$, $\mu_{20} = \alpha_{10}\alpha_{20} + \alpha_{01}\beta_{20} - \beta_{11}\alpha_{10} - \frac{\alpha_{11}\alpha_{10}^2}{\alpha_{01}}$, $\mu_{11} = \beta_{11} + \frac{\alpha_{10}\alpha_{11}}{\alpha_{01}}$, and \tilde{P}_1, \tilde{P}_2 are the power series in (U_1, U_2) with powers U_1^i, U_2^j satisfying $i + j \geq 3$.

Next, under the following C^∞ change of coordinates in the close vicinity of $(0, 0)$.

Define $V_1 = U_1$, $V_2 = \xi_{00} + U_2 + \xi_{20}U_1^2 + \xi_{11}U_1U_2$, system (15) reduced to

$$\begin{cases} \frac{dV_1}{dt} = V_2 + \check{P}_1(V_1, V_2), \\ \frac{dV_2}{dt} = \gamma_{00} + \gamma_{10}V_1 + \gamma_{01}V_2 + \gamma_{20}V_1^2 + \gamma_{11}V_1V_2 + \gamma_{02}V_2^2 + \check{P}_2(V_1, V_2), \end{cases} \quad (16)$$

where $\gamma_{00} = \mu_{00} - \mu_{01}\xi_{00}$, $\gamma_{10} = \mu_{10} - \mu_{11}\xi_{00} + \xi_{11}\mu_{00} - \mu_{01}\xi_{00}\xi_{11}$, $\gamma_{01} = \mu_{01} - \xi_{11}\xi_{00}$, $\gamma_{20} = \mu_{20} - \mu_{01}\xi_{20} + \xi_{11}\mu_{10} - \mu_{11}\xi_{00}\xi_{11}$, $\gamma_{11} = 2\xi_{20} + \mu_{11} - \mu_{01}\xi_{11} + \xi_{11}\mu_{01}$, $\gamma_{02} = \xi_{11}$, and \check{P}_1, \check{P}_2 are the power series in (V_1, V_2) with powers V_1^i, V_2^j satisfying $i + j \geq 3$.

Let us introduce a new time variable T by $dt = (1 - \gamma_{02}V_1)dT$. Rewriting T as t , the system (16) can be rewritten as

$$\begin{cases} \frac{dV_1}{dt} = V_2(1 - \gamma_{02}V_1) + \check{P}_1(V_1, V_2), \\ \frac{dV_2}{dt} = (1 - \gamma_{02}V_1)[\gamma_{00} + \gamma_{10}V_1 + \gamma_{01}V_2 + \gamma_{20}V_1^2 + \gamma_{11}V_1V_2 + \gamma_{02}V_2^2 + \check{P}_2(V_1, V_2)], \end{cases} \quad (17)$$

$Z_1 = V_1, Z_2 = V_2(1 - \gamma_{02}V_1) + \check{P}_1(V_1, V_2)$, then system (17) reduced to

$$\begin{cases} \frac{dZ_1}{dt} = Z_2, \\ \frac{dZ_2}{dt} = \delta_{00} + \delta_{10}Z_1 + \delta_{01}Z_2 + \delta_{20}Z_1^2 + \delta_{11}Z_1Z_2 + \bar{P}_2(Z_1, Z_2), \end{cases} \quad (18)$$

where $\delta_{00} = \gamma_{00}, \delta_{10} = \gamma_{10} - 2\gamma_{02}\gamma_{00}, \delta_{01} = \gamma_{01}, \delta_{20} = \gamma_{20} + \gamma_{00}\gamma_{02}^2 - 2\gamma_{02}\gamma_{10}, \delta_{11} = \gamma_{11} - \gamma_{02}\gamma_{01}$, and \bar{P}_2 are the power series in (Z_1, Z_2) with powers Z_1^i, Z_2^j satisfying $i + j \geq 3$.

One can not determine the sign of δ_{20} whenever $\lambda_1 \rightarrow 0$ and $\lambda_2 \rightarrow 0$. Consequently, it is essential to consider the following two cases:

Case 1: $\delta_{20} > 0$, Consider $u_1 = Z_1, u_2 = \frac{Z_2}{\sqrt{\delta_{20}}}, d\tau = \sqrt{\delta_{20}}dt$, then system (18) becomes

$$\begin{cases} \frac{du_1}{d\tau} = u_2, \\ \frac{du_2}{d\tau} = \frac{\delta_{00}}{\delta_{20}} + \frac{\delta_{10}}{\delta_{20}}u_1 + \frac{\delta_{01}}{\sqrt{\delta_{20}}}u_2 + u_1^2 + \frac{\delta_{11}}{\sqrt{\delta_{20}}}u_1u_2 + P(u_1, u_2, \lambda), \end{cases} \quad (19)$$

where $P(u_1, u_2, 0)$ is a power series in (u_1, u_2) with powers u_1^i, u_2^j satisfying $i + j \geq 3$.

Using the affine transformation $v_1 = u_1 + \frac{\delta_{10}}{2\delta_{20}}, v_2 = u_2$, then system (19) becomes

$$\begin{cases} \frac{dv_1}{d\tau} = v_2, \\ \frac{dv_2}{d\tau} = \frac{\delta_{00}}{\delta_{20}} - \frac{\delta_{10}^2}{4\delta_{20}^2} + \left(\frac{\delta_{01}}{\sqrt{\delta_{20}}} - \frac{\delta_{11}\delta_{10}}{2\delta_{20}\sqrt{\delta_{20}}} \right)v_2 + v_1^2 + \frac{\delta_{11}}{\sqrt{\delta_{20}}}v_1v_2 + Q(v_1, v_2, \lambda), \end{cases} \quad (20)$$

where $Q(v_1, v_2, 0)$ is a power series in (v_1, v_2) with powers v_1^i, v_2^j satisfying $i + j \geq 3$.

Consider $w_1 = \frac{\delta_{11}^2}{\delta_{20}}v_1, w_2 = \frac{\delta_{11}^3}{\delta_{20}\sqrt{\delta_{20}}}v_2, t = \frac{\sqrt{\delta_{20}}}{\delta_{11}}\tau$, then the system (20) becomes

$$\begin{cases} \frac{dw_1}{dt} = w_2, \\ \frac{dw_2}{dt} = v_1(\lambda_1, \lambda_2) + v_2(\lambda_1, \lambda_2)w_2 + w_1^2 + w_1w_2 + R(w_1, w_2, \lambda), \end{cases}$$

where $v_1(\lambda_1, \lambda_2) = \frac{\delta_{00}\delta_{11}^4}{\delta_{20}^3} - \frac{\delta_{10}^2\delta_{11}^4}{4\delta_{20}^4}, v_2(\lambda_1, \lambda_2) = \frac{\delta_{01}\delta_{11}}{\delta_{20}} - \frac{\delta_{11}^2\delta_{10}}{2\delta_{20}^2}$, and $R(w_1, w_2, 0)$ is a power series in (w_1, w_2) with powers w_1^i, w_2^j satisfying $i + j \geq 3$.

Case 2: $\delta_{20} < 0$, Consider $\bar{u}_1 = z_1, \bar{u}_2 = \frac{z_2}{\sqrt{-\delta_{20}}}, d\tau = \sqrt{-\delta_{20}}dt$, then system (18) becomes

$$\begin{cases} \frac{d\bar{u}_1}{d\tau} = \bar{u}_2, \\ \frac{d\bar{u}_2}{d\tau} = \frac{-\delta_{00}}{\delta_{20}} - \frac{\delta_{10}}{\delta_{20}}\bar{u}_1 + \frac{\delta_{01}}{\sqrt{-\delta_{20}}}\bar{u}_2 - \bar{u}_1^2 + \frac{\delta_{11}}{\sqrt{-\delta_{20}}}\bar{u}_1\bar{u}_2 + \bar{P}(\bar{u}_1, \bar{u}_2, \lambda), \end{cases} \quad (21)$$

where $\bar{P}(\bar{u}_1, \bar{u}_2, 0)$ is a power series in (\bar{u}_1, \bar{u}_2) with powers \bar{u}_1^i, \bar{u}_2^j satisfying $i + j \geq 3$.

Using the affine transformation $\bar{v}_1 = \bar{u}_1 + \frac{\delta_{10}}{2\delta_{20}}, \bar{v}_2 = \bar{u}_2$, then system (21) becomes

$$\begin{cases} \frac{d\bar{v}_1}{d\tau} = \bar{v}_2, \\ \frac{d\bar{v}_2}{d\tau} = -\frac{\delta_{00}}{\delta_{20}} + \frac{\delta_{10}^2}{4\delta_{20}^2} + \left(\frac{\delta_{01}}{\sqrt{-\delta_{20}}} - \frac{\delta_{11}\delta_{10}}{2\delta_{20}\sqrt{-\delta_{20}}} \right)\bar{v}_2 + \bar{v}_1^2 + \frac{\delta_{11}}{\sqrt{-\delta_{20}}}\bar{v}_1\bar{v}_2 + \bar{Q}(\bar{v}_1, \bar{v}_2, \lambda), \end{cases} \quad (22)$$

where $\bar{Q}(\bar{v}_1, \bar{v}_2, 0)$ is a power series in (\bar{v}_1, \bar{v}_2) with powers \bar{v}_1^i, \bar{v}_2^j satisfying $i + j \geq 3$.

Consider $\bar{w}_1 = \frac{\delta_{11}^2}{\delta_{20}} \bar{v}_1$, $\bar{w}_2 = -\frac{\delta_{11}^3}{\delta_{20}\sqrt{-\delta_{20}}} \bar{v}_2$, $t = -\frac{\sqrt{-\delta_{20}}}{\delta_{11}} \tau$, then system (22) becomes

$$\begin{cases} \frac{d\bar{w}_1}{dt} = \bar{w}_2, \\ \frac{d\bar{w}_2}{dt} = \bar{v}_1(\lambda_1, \lambda_2) + \bar{v}_2(\lambda_1, \lambda_2)\bar{w}_2 + \bar{w}_1^2 + \bar{w}_1\bar{w}_2 + \bar{R}(\bar{w}_1, \bar{w}_2, \lambda), \end{cases} \quad (23)$$

where $\bar{v}_1(\lambda_1, \lambda_2) = \frac{\delta_{00}\delta_{11}^4}{\delta_{20}^3} - \frac{\delta_{10}^2\delta_{11}^4}{4\delta_{20}^4}$, $\bar{v}_2(\lambda_1, \lambda_2) = \frac{\delta_{01}\delta_{11}}{\delta_{20}} - \frac{\delta_{11}^2\delta_{10}}{2\delta_{20}^2}$, and $\bar{R}(\bar{w}_1, \bar{w}_2, 0)$ is a power series in (\bar{w}_1, \bar{w}_2) with powers \bar{w}_1^i, \bar{w}_2^j satisfying $i + j \geq 3$.

In order to minimize the number of cases, it is advisable to retain $v_1(\lambda)$ and $v_2(\lambda)$ to denote $\bar{v}_1(\lambda)$, and $\bar{v}_2(\lambda)$ in system (23). Moreover, if $\left| \frac{\partial(v_1, v_2)}{\partial(\lambda_1, \lambda_2)} \right|_{\lambda_1=\lambda_2=0} \neq 0$, then the parameter transformations

$$v_1(\lambda_1, \lambda_2) = \frac{\delta_{00}\delta_{11}^4}{\delta_{20}^3} - \frac{\delta_{10}^2\delta_{11}^4}{4\delta_{20}^4}, \quad v_2(\lambda_1, \lambda_2) = \frac{\delta_{01}\delta_{11}}{\delta_{20}} - \frac{\delta_{11}^2\delta_{10}}{2\delta_{20}^2},$$

and

$$\bar{v}_1(\lambda_1, \lambda_2) = \frac{\delta_{00}\delta_{11}^4}{\delta_{20}^3} - \frac{\delta_{10}^2\delta_{11}^4}{4\delta_{20}^4}, \quad \bar{v}_2(\lambda_1, \lambda_2) = \frac{\delta_{01}\delta_{11}}{\delta_{20}} - \frac{\delta_{11}^2\delta_{10}}{2\delta_{20}^2},$$

are topologically equivalent in the vicinity of the origin and v_1, v_2 are independent parameters. As a result, it can be inferred that the system (13) experiences the Bogdanov-Takens bifurcation when the values of (λ_1, λ_2) are within closed proximity to the origin $(0, 0)$, [38]. The following are the local representations of the bifurcation curves:

- 1 The Saddle-node bifurcation curve $SN = \{(v_1, v_2) : v_1 = 0, v_2 \neq 0\}$.
- 2 The Hopf bifurcation curve $H = \{(v_1, v_2) : v_2 = \pm\sqrt{-v_1}, v_1 < 0\}$.
- 3 The Homoclinic bifurcation curve $HL = \{(v_1, v_2) : v_2 = \pm\sqrt[5]{-v_1}, v_1 < 0\}$.

6 Numerical simulation

In this section, numerical simulations are provided to validate our analytical findings. We benefited from MATHEMATICA 10.0 software to draw the phase portrait diagrams for the computations. We provide a total of six numerical examples, each carefully selected to demonstrate the implications of our analytical results. For these examples, we have chosen specific values for the ecosystem parameters $\gamma, \beta, \xi, \delta$, and θ to ensure that they align with the theoretical findings and enhance the understanding of the dynamics of the systems.

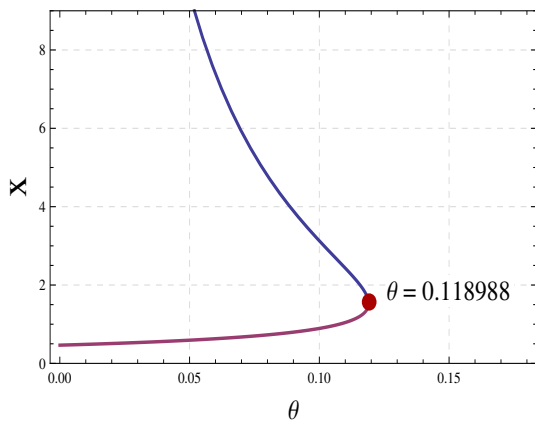
(1)

$$\begin{cases} \frac{dx}{dt} = x \left(\left(1 - \frac{x}{5}\right) - \frac{y}{1+2.8 \times 0.35+x} \right), \\ \frac{dy}{dt} = y \left(\frac{0.9(x+0.35)}{1+2.8 \times 0.35+x} - 0.3 - \theta x \right). \end{cases} \quad (24)$$

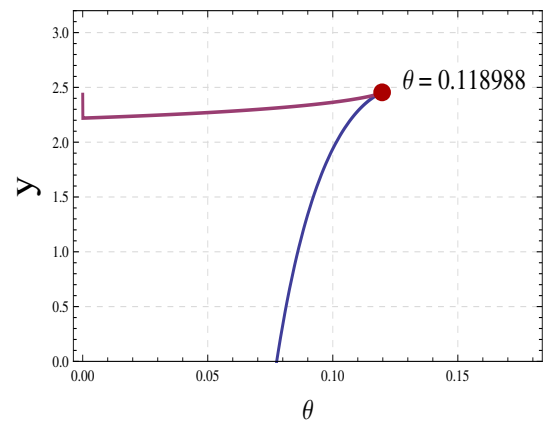
System (24) exhibits several equilibrium points depending on parametric conditions. The nature of these points is explained in Table 1 and is also depicted in Figure 1. A threshold value of the anti-predator behavior parameter $\theta = 0.118988$ is obtained in Figure 1a and Figure 1b.

Table 1. Number and nature of equilibrium points (Eps) of the system (24)

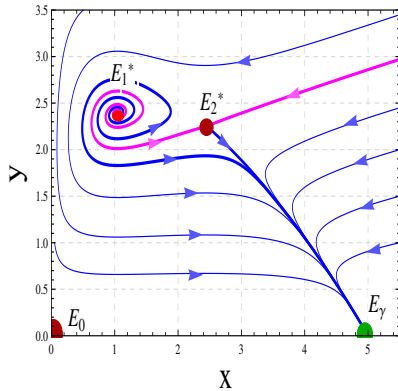
Value of θ	Conditions	Number of Eps	Existence of Eps	Nature of Eps	Figure
$0 < \theta < 0.118988$	$\Delta_2^2 > \Delta_3$	4	$E_0 = (0,0)$ $E_\gamma = (5,0)$ $E_1^* = (1.04319, 2.39244)$ $E_2^* = (2.43136, 2.26624)$	Saddle Stable Unstable Saddle	1c
$\theta = 0.11898$	$\Delta_2^2 = \Delta_3$	3	$E_0 = (0,0)$ $E_\gamma = (5,0)$ $E_3^* = (1.53127, 2.43593)$	Saddle Stable Unstable saddle-node	1d
$\theta > 0.11898$	$\Delta_2^2 < \Delta_3$	2	$E_0 = (0,0)$ $E_\gamma = (5,0)$	Saddle Globally Stable	1e



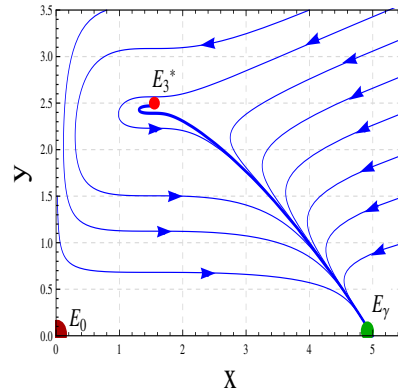
(a)



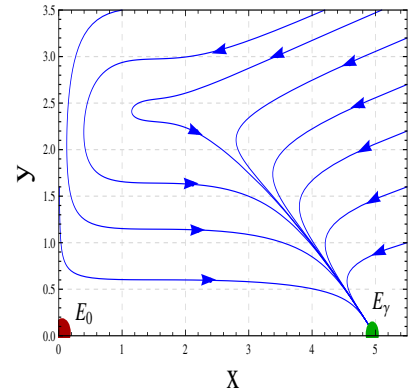
(b)



(c)



(d)



(e)

Figure 1. (a)-(b) Saddle-node bifurcation diagram. (c) $\theta = 0.11$. The equilibrium point E_1^* is unstable, and E_2^* is a saddle. (d) $\theta = 0.118988$. The equilibrium point E_3^* is an unstable saddle node. (e) $\theta = 0.12$. The predator-free equilibrium point is globally stable. Ecologically, there is a threshold value of the anti-predator parameter θ below which species may coexist and above which the predator species go extinct, leading to the collapse of the system

(2)

$$\begin{cases} \frac{dx}{dt} = x \left(\left(1 - \frac{x}{2}\right) - \frac{y}{1+0.001 \times 0.8+x} \right), \\ \frac{dy}{dt} = y \left(\frac{0.4(x+0.8)}{1+0.001 \times 0.8+x} - 0.3 - 0.11x \right). \end{cases} \quad (25)$$

Table 2. Number and nature of equilibrium points (Eqs) of the system (25)

Condition	Number of Eqs	Existence of Eqs	Nature of Eqs	Figure
$\Delta_1 < 0$	3	$E_0 = (0,0)$ $E_\gamma = (2,0)$ $E_4^* = (0.380454, 1.1185)$	Unstable Stable Saddle	2

Table 3. Number and nature of equilibrium points (Eqs) of the system (26)

Value of θ	Conditions	Number of Eqs	Existence of Eqs	Nature of Eqs	Figure
$\theta = 0.2$	$\Delta_1 = 0, \Delta_2 > 0,$	4	$E_0 = (0,0)$ $E_\gamma = (3,0)$ $E_5^* = (1.992, 1.008)$ $E_6^* = (0, 1.02)$	Unstable Stable Saddle Unstable saddle node	3a
$\theta = 0.8$	$\Delta_1 = 0, \Delta_2 < 0,$	3	$E_0 = (0,0)$ $E_\gamma = (3,0)$ $E_6^* = (0, 1.008)$	Unstable Stable Cusp	3b

System (25) exhibits several equilibrium points depending on the parametric condition. The nature of these points is explained in Table 2 and is also shown graphically in Figure 2.

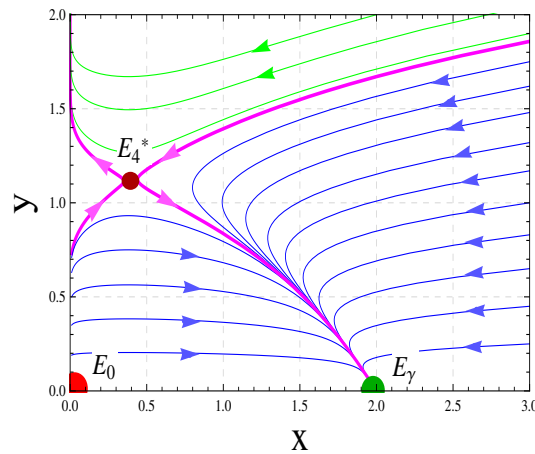


Figure 2. The equilibrium point E_0 is unstable, E_γ is stable, and E_4^* is saddle. Ecologically, the system will collapse due to the extinction of either the prey or the predator

(3)

$$\begin{cases} \frac{dx}{dt} = x \left(\left(1 - \frac{x}{3}\right) - \frac{y}{1+0.02381 \times 0.336+x} \right), \\ \frac{dy}{dt} = y \left(\frac{0.9(x+0.336)}{1+0.02381 \times 0.336+x} - 0.3 - \theta x \right). \end{cases} \tag{26}$$

System (26) exhibits several equilibrium points depending on certain parametric conditions. The nature of these points is explained in Table 3 and is also shown graphically in Figure 3.

(4)

$$\begin{cases} \frac{dx}{dt} = x \left(\left(1 - \frac{x}{\gamma}\right) - \frac{y}{1+2.8 \times 0.35+x} \right), \\ \frac{dy}{dt} = y \left(\frac{0.9(x+0.35)}{1+2.8 \times 0.35+x} - 0.3 - 0.11x \right), \end{cases} \tag{27}$$

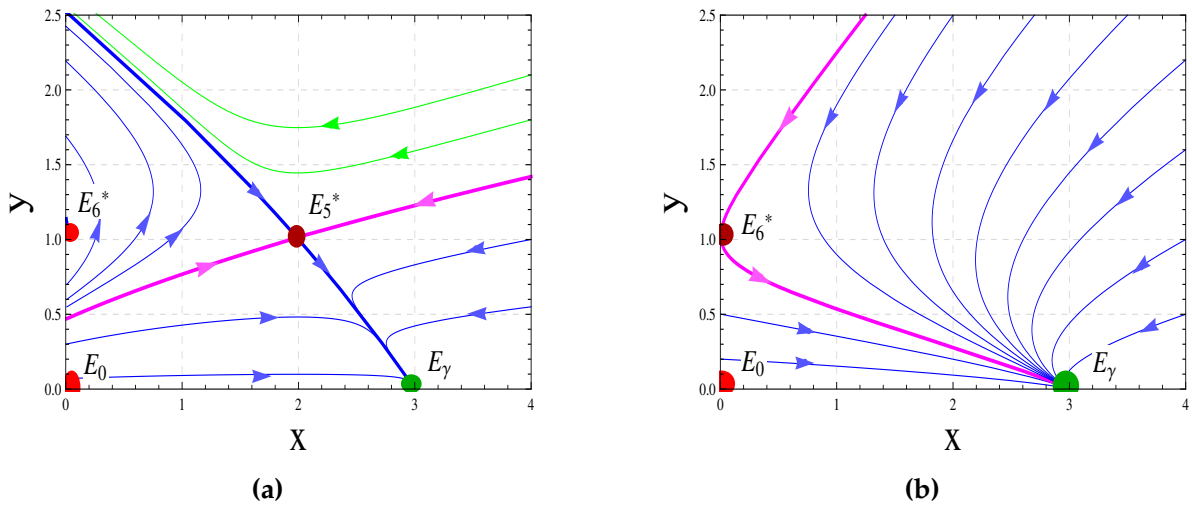


Figure 3. (a) $\theta = 0.2$. The equilibrium point E_0 is unstable, E_γ is globally stable, E_5^* is a saddle point, and E_6^* is an unstable saddle node. (b) $\theta = 0.8$. The equilibrium point E_0 is unstable, E_γ is globally stable, and E_6^* forms a cusp of co-dimension 2. Ecologically, the system will collapse

Table 4. Number and nature of feasible equilibrium points (Eqs) of the system (27)

Value of γ	Existence of Eqs	Nature of Eqs	Figure
$\gamma = 3.5$	$E_0 = (0, 0)$ $E_\gamma = (3.5, 0)$ $E_1^*(1.04319, 2.12212)$ $E_2^*(2.43136, 1.3469)$	Saddle Stable Stable Saddle	4a
$\gamma = 4.06638$	$E_0 = (0, 0)$ $E_\gamma = (4.06638, 0)$ $E_1^*(1.04319, 2.24762)$ $E_2^*(2.43136, 1.77373)$	Saddle Stable Stable limit cycle Saddle	4b
$\gamma = 4.61$	$E_0 = (0, 0)$ $E_\gamma = (4.61, 0)$ $E_1^*(1.04319, 2.33908)$ $E_2^*(2.43136, 2.08477)$	Saddle Stable Homoclinic loop Saddle	4c
$\gamma = 5$	$E_0 = (0, 0)$ $E_\gamma = (5, 0)$ $E_1^*(1.04319, 2.39244)$ $E_2^*(2.43136, 2.26624)$	Saddle Stable Unstable Saddle	4d

The system (27) exhibits several equilibrium points depending on the value of γ . The nature of these points is explained in Table 4 and is also shown graphically in Figure 4.

(5)

$$\begin{cases} \frac{dx}{dt} = x \left(\left(1 - \frac{x}{\gamma}\right) - \frac{y}{1+2.8 \times 0.35+x} \right), \\ \frac{dy}{dt} = y \left(\frac{0.9(x+0.35)}{1+2.8 \times 0.35+x} - 0.3 - 0.118988x \right). \end{cases} \quad (28)$$

System (28) exhibits several equilibrium points depending on certain parametric conditions. The nature of these points is explained in Table 5 and is also shown graphically in Figure 5.

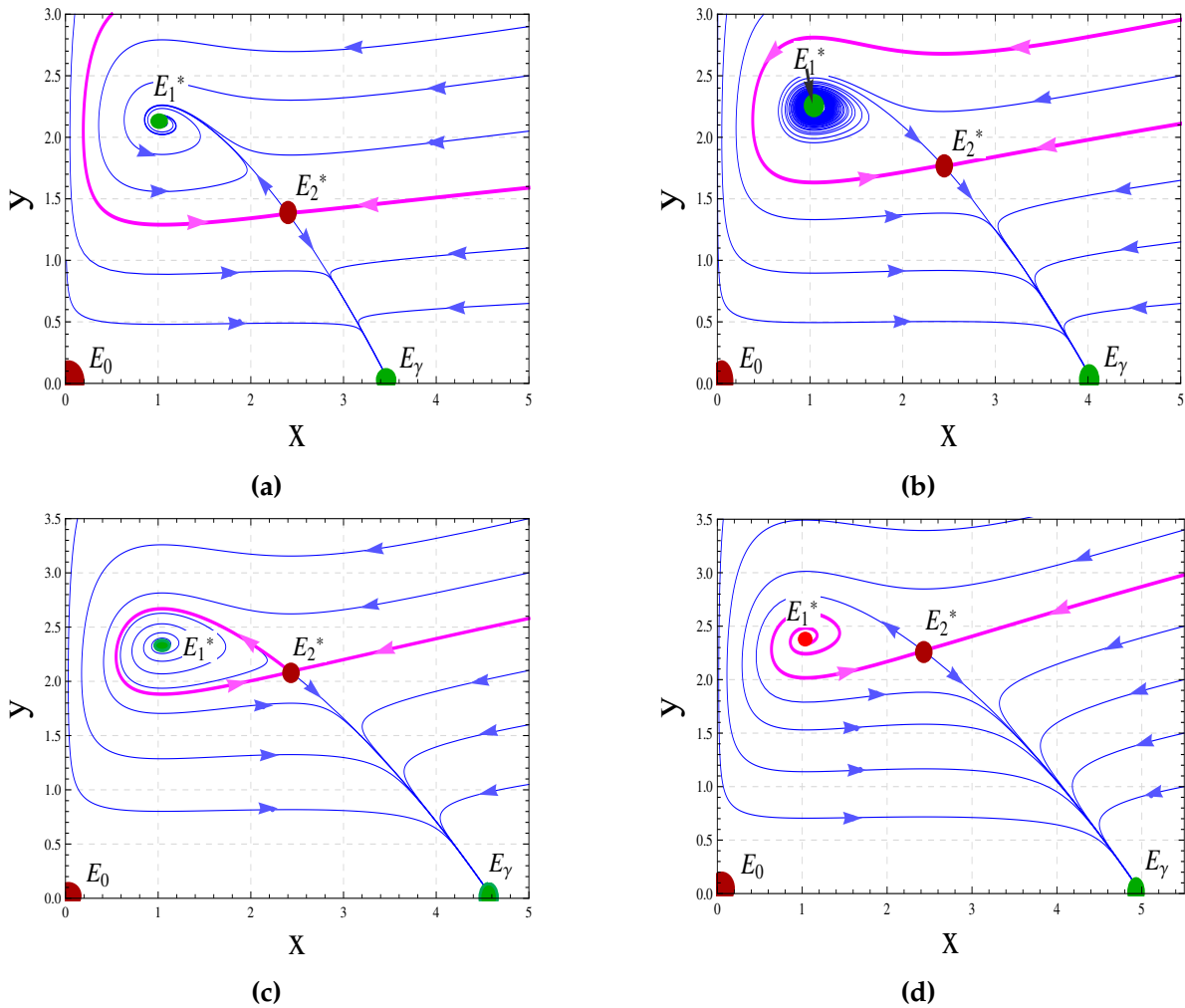


Figure 4. (a) $\gamma = 3.5$. The equilibrium point $E_1^* = (1.04319, 2.12212)$ is a stable point. (b) $\gamma = \gamma^{[hf]} = 4.06638$. A stable limit cycle arises around the point $E_1^*(1.04319, 2.24762)$. (c) $\gamma = 4.61$. The limit cycle collides with the saddle point, $E_2^* = (2.43136, 2.08477)$ and consequently a homoclinic loop arises around the point $E_1^*(1.04319, 2.33908)$. (d) $\gamma = 5$. The equilibrium $E_1^* = (1.04319, 2.39244)$ is an unstable point. Ecologically, the system will either stabilise or collapse, contingent upon the parametric conditions and the initial population of the species

Table 5. Nature of equilibrium points of the system (28)

Value of γ	Conditions	Existence of Eqs	Nature of Eqs	Figure
$\gamma = 3$	$\gamma < 1 + \alpha\zeta + 2u_1^*$	$E_0 = (0, 0)$ $E_\gamma = (3, 0)$ $E_3^*(1.53127, 1.71904)$	Saddle Stable Stable saddle-node	5a
$\gamma = 5.04253$	$\gamma = 1 + \alpha\zeta + 2u_1^*$	$E_0 = (0, 0)$ $E_\gamma = (5.04253, 0)$ $E_3^*(1.53127, 2.445)$	Saddle Stable Cusp	5b
$\gamma = 5.2$	$\gamma > 1 + \alpha\zeta + 2u_1^*$	$E_0 = (0, 0)$ $E_\gamma = (5.2, 0)$ $E_3^*E_3^*(1.53127, 2.47729)$	Saddle Stable Unstable saddle-node	5c

(6)

$$\begin{cases} \frac{dx}{dt} = x \left(\left(1 - \frac{x}{3.2777 + \lambda_1} \right) - \frac{y}{1 + 2.5 \times 0.25 + x} \right) = f_1(x, y, \lambda_1), \\ \frac{dy}{dt} = y \left(\frac{0.8(x + 0.25)y}{1 + 2.5 \times 0.25 + x} - 0.2 - (0.183055 + \lambda_2)x \right) = f_2(x, y, \lambda_2). \end{cases} \quad (29)$$

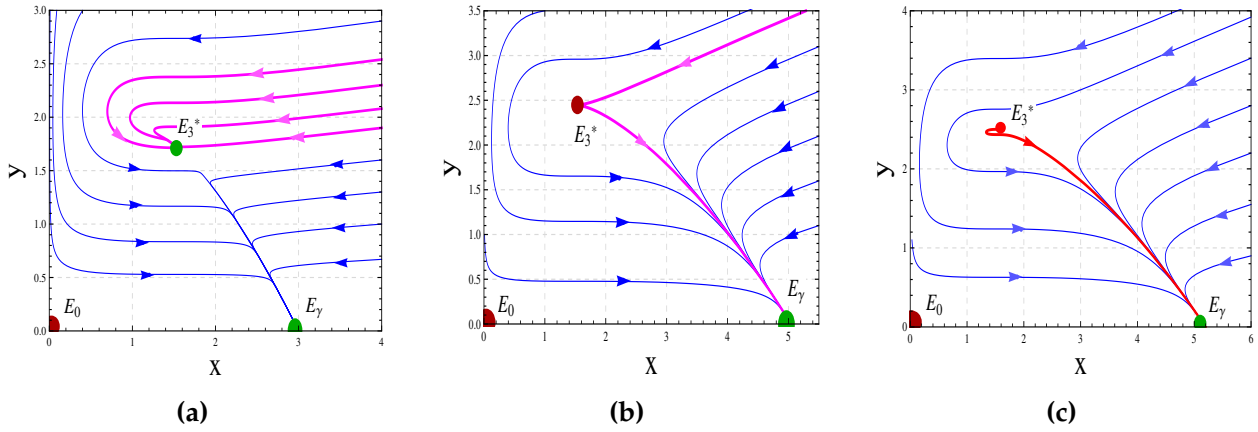


Figure 5. (a) $\gamma = 3$. The equilibrium point $E_3^*(1.53127, 1.71904)$ is a stable saddle-node. (b) $\gamma = 5.04253$. The equilibrium point $E_3^*(1.53127, 2.445)$ is a cusp of co-dimension 2. (c) $\gamma = 5.2$. The equilibrium point $E_3^*(1.53127, 2.47729)$ is an unstable saddle-node. Ecologically, the system will either stabilise or collapse, contingent upon the parametric conditions and the initial population of the species

The system (29) has a unique interior equilibrium point $E_3^* = (0.82635, 1.83333)$. The transformations $U = x - 0.82635$, $V = y - 1.83333$ are used to move the point $E_3^* = (0.82635, 1.83333)$ to the origin and next, the affine transformation $U_1 = U$, $U_2 = \alpha_{10}U + \alpha_{01}V$ is introduced. The system (29) shrinks to

$$\begin{cases} \frac{dU_1}{dt} = \zeta_{00} + U_2 + \zeta_{20}U_1^2 + \zeta_{11}U_1U_2 + \tilde{P}_1(U_1, U_2), \\ \frac{dU_2}{dt} = \mu_{00} + \mu_{10}U_1 + \mu_{01}U_2 + \mu_{20}U_1^2 + \mu_{11}U_1U_2 + \tilde{P}_2(U_1, U_2), \end{cases} \quad (30)$$

where $\zeta_{00} = 0.82635 \left(0.252113 - \frac{0.82635}{3.2777 + \lambda_1} \right)$, $\zeta_{20} = 0.202246 - \frac{1}{3.2777 + \lambda_1} - 0.802203 \left(0.504225 - \frac{1.6527}{3.2777 + \lambda_1} \right)$, $\zeta_{11} = 0.802203$, $\mu_{00} = 0.82635 \left(0.504225 - \frac{1.6527}{3.2777 + \lambda_1} \right) \left(0.252113 - \frac{0.82635}{3.2777 + \lambda_1} \right) + 0.510698\lambda_2$, $\mu_{10} = 1.833330 \left(0.504225 - \frac{1.6527}{3.2777 + \lambda_1} \right) \lambda_2 - 0.3371 \left(0.335601 - 1.83333(0.183055 + \lambda_2) \right)$, $\mu_{01} = 0.504225 - \frac{1}{3.2777 + \lambda_1} - 1.83333\lambda_2$, $\mu_{20} = 0.0461505 - 0.802203 \left(0.504225 - \frac{1.6527}{3.2777 + \lambda_1} \right)^2 + \left(0.504225 - \frac{1.6527}{3.2777 + \lambda_1} \right) \left(0.202246 - \frac{1}{3.2777 + \lambda_1} \right) - \left(0.504225 - \frac{1.6527}{3.2777 + \lambda_1} \right) \left(-8.32667 \times 10^{-17} - \lambda_2 \right)$, $\mu_{11} = -8.32667 \times 10^{-17} + 0.802203 \left(0.504225 - \frac{1.6527}{3.2777 + \lambda_1} \right) - \lambda_2$,

and \tilde{P}_1, \tilde{P}_2 are the power series in (x_1, x_2) with powers x_1^i, x_2^j satisfying $i + j \geq 3$.

Consider the C^∞ change of co-ordinates in the close vicinity of $(0, 0)$: $V_1 = U_1$, $V_2 = \zeta_{00} + U_2 + \zeta_{20}U_1^2 + \zeta_{11}U_1U_2$, $dt = (1 - \gamma_{02}V_1)dT$ and $Z_1 = V_1, Z_2 = V_2(1 - \gamma_{02}V_1) + \tilde{P}_1(V_1, V_2)$ respectively. The system (30) shrinks to

$$\begin{cases} \frac{dZ_1}{dt} = Z_2, \\ \frac{dZ_2}{dt} = \delta_{00} + \delta_{10}Z_1 + \delta_{01}Z_2 + \delta_{20}Z_1^2 + \delta_{11}Z_1Z_2 + \tilde{P}_2(Z_1, Z_2), \end{cases} \quad (31)$$

where $\delta_{00} = \frac{5.48659\lambda_2 + 4.59973\lambda_1\lambda_2 + 0.892642\lambda_1^2\lambda_2}{(3.2777 + \lambda_1)^2}$,

$\delta_{10} = \frac{6.0311 \times 10^{-16} + 3.5065 \times 10^{-16}\lambda_1 - 0.084269\lambda_1^2 + 2.23819\lambda_2 + 4.07424\lambda_1\lambda_2 + 1.03468\lambda_1^2\lambda_2}{(3.2777 + \lambda_1)^2}$,

$\delta_{01} = \frac{-4.42835 \times 10^{-16} + 0.3371\lambda_1 - 6.00912\lambda_2 - 1.83333\lambda_1\lambda_2}{3.2777 + \lambda_1}$,

Table 6. Nature of equilibrium points

Region	Behavior of the region
Region I	Number interior points
Region II	Two interior points, one is saddle and the other is stable
Region III	Two interior points, one is saddle and the other is stable enclosed by a limit cycle
Region IV	Two interior points, one is saddle and the other is unstable

$$\delta_{11} = \frac{-0.6742 - 0.270422\lambda_1 + 1.54283\lambda_2 + 0.470705\lambda_1\lambda_2}{3.2777 + \lambda_1},$$

$$\delta_{20} = \frac{0.49581 + 0.302535\lambda_1 + 0.113751\lambda_1^2 - 10.8827\lambda_2 - 9.36911\lambda_1\lambda_2 - 1.84547\lambda_1^2\lambda_2}{(3.2777 + \lambda_1)^2} \text{ and } \bar{P}_2 \text{ are the power series}$$

in (z_1, z_2) with powers z_1^i, z_2^j satisfying $i + j \geq 3$. Thus $\delta_{20} = 0.0461505 > 0$. By using the following three transformations:

$$(i) \quad u_1 = Z_1, \quad u_2 = \frac{Z_2}{\sqrt{\delta_{20}}}, \quad d\tau = \sqrt{\delta_{20}} dt,$$

$$(ii) \quad v_1 = u_1 + \frac{\delta_{10}}{2\delta_{20}}, \quad v_2 = u_2,$$

$$(iii) \quad w_1 = \frac{\delta_{11}^2}{\delta_{20}} v_1, \quad w_2 = \frac{\delta_{11}^3}{\delta_{20}\sqrt{\delta_{20}}} v_2, \quad t = \frac{\sqrt{\delta_{20}}}{\delta_{11}} \tau,$$

system (31) shrinks to

$$\begin{cases} \frac{dw_1}{dt} = w_2, \\ \frac{dw_2}{dt} = v_1(\lambda_1, \lambda_2) + v_2(\lambda_1, \lambda_2)w_2 + w_1^2 + w_1w_2 + R(w_1, w_2, \lambda), \end{cases}$$

where $v_1(\lambda_1, \lambda_2) = \frac{\delta_{00}\delta_{11}^4}{\delta_{20}^3} - \frac{\delta_{10}^2\delta_{11}^4}{4\delta_{20}^4}$ and $v_2(\lambda_1, \lambda_2) = \frac{\delta_{01}\delta_{11}}{\delta_{20}} - \frac{\delta_{11}^2\delta_{10}}{2\delta_{20}^2}$. The determinant of the matrix $\left[\frac{\partial(v_1, v_2)}{\partial(\lambda_1, \lambda_2)} \right]_{\lambda_1=\lambda_2=0} = -5.35162 \times 10^{-6} \neq 0$. The rank of matrix $\left[\frac{\partial(v_1, v_2)}{\partial(\lambda_1, \lambda_2)} \right]_{\lambda_1=\lambda_2=0}$ is 2 as a result,

$v_1(\lambda_1, \lambda_2) = \frac{\delta_{00}\delta_{11}^4}{\delta_{20}^3} - \frac{\delta_{10}^2\delta_{11}^4}{4\delta_{20}^4}$, $v_2(\lambda_1, \lambda_2) = \frac{\delta_{01}\delta_{11}}{\delta_{20}} - \frac{\delta_{11}^2\delta_{10}}{2\delta_{20}^2}$ are non-singular parameter transformations. In the $\lambda_1\lambda_2$ plane, the three bifurcation curves separate the local neighborhood of the BT-bifurcation point $(0, 0)$ into four distinct regions: Region I, Region II, Region III, and Region IV, as illustrated in Figure 6a. The saddle-node bifurcation curve is represented in red, the Hopf bifurcation curve in blue, and the homoclinic bifurcation curve in green. The system (29) has a unique interior equilibrium point that is a cusp of co-dimension 2 when $\lambda_1 = 0 = \lambda_2$, as seen in Figure 6b. When the values of λ_1 and λ_2 vary and they belong to region I, the predator species in this region are likely to face extinction due to the absence of an interior equilibrium point, as seen in Figure 6c. When the values of λ_1 and λ_2 belong to region II, there are two interior equilibrium points. Among these equilibrium points, one exhibits the characteristics of a saddle, while the other demonstrates stability. Therefore, it can be inferred that the initial population size will play a crucial role in determining the possibility of the coexistence of the two species or the ultimate extinction of the predator species, as seen in Figure 6d. When the values of λ_1 and λ_2 belong to the region III, the stable equilibrium point loses its stability, and a stable limit cycle emerges around this point. Therefore, it can be inferred that the initial population size will play a crucial role in determining the possibility of oscillation, or the predator species tends to become extinct as seen in Figure 6e. When the values of λ_1 and λ_2 belong to the region IV, the limit cycle will disappear and there will be an unstable focus and saddle point. Therefore, it can be inferred that the predator species go extinct, as seen in Figure 6f.

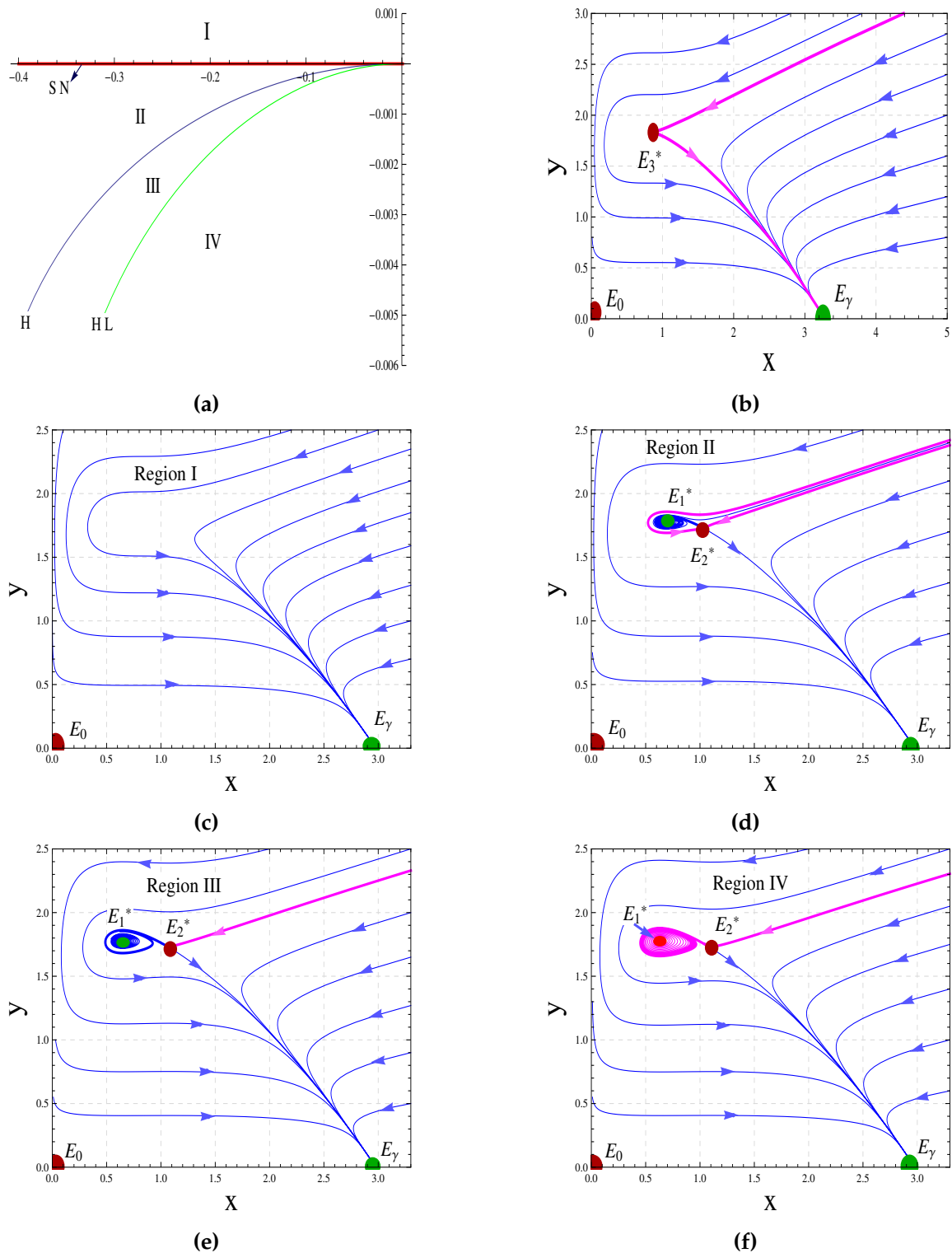


Figure 6. (a) Bifurcation diagram of the model (3). The saddle-node bifurcation curve is shown in red, the Hopf bifurcation curve in blue, and the homoclinic bifurcation curve in green. (b) The unique interior equilibrium point E_3^* , when $\lambda_1 = \lambda_2 = 0$ is a cusp of co-dimension 2. (c) When $(\lambda_1, \lambda_2) = (-0.3, 0.0003)$ lies in region I, the system (3) has no interior equilibrium point and the equilibrium point E_γ is globally asymptotically stable. (d) When $(\lambda_1, \lambda_2) = (-0.3, -0.002)$ lies in the region II, system (3) has two interior equilibrium points. One is a saddle, while the other is stable. (e) When $(\lambda_1, \lambda_2) = (-0.3, -0.004)$ lies in the region III, a stable limit cycle enclosing an interior point, and the other interior point is a saddle, system (3) has two interior equilibrium points. (f) When $(\lambda_1, \lambda_2) = (-0.3, -0.0048)$ lies in the region IV, system (3) has two interior equilibrium points: one is a saddle, while the other is an unstable one. Ecologically, system (3) is highly sensitive to the parameters θ and γ . A slight variation in these parameters can lead to significant changes in the system's dynamics, such as species coexistence, coexistence through oscillations, or the extinction of the predator species

7 Impact of Anti-predator behavior

The proposed model (3) without anti-predator behavior has been analyzed by Srinivasu et al. [8]. The authors observed some interesting results, which are very important from an ecological point of view. In this section, we aim to discuss how the anti-predator parameter θ affects the dynamics of the proposed system. In Figure 7a, Figure 7b, Figure 7c and Figure 7d we have depicted the region of coexistence. In Figure 7a, only parameters θ (anti-predator) and ξ (quantity of additional food) are allowed to vary. In Figure 7b, only parameters θ (anti-predator) and α (quality of additional food) are allowed to vary. In Figure 7c, only parameters θ (anti-predator) and δ (ratio of the predator’s mortality rate and prey growth rate) are allowed to vary. In Figure 7d, only parameters θ (anti-predator) and parameter β (ratio of nutritional value of prey to the product of prey’s handling time and prey growth rate) are allowed to vary. These graphs play a vital role in examining the range of parameter θ as the other parameters vary. In Figure 8, we have plotted the time series solution graphs where all the parameters of the model are fixed except θ . It can be observed that as θ increases, the periodicity of solutions decreases, and eventually, the solutions become non-periodic solutions.

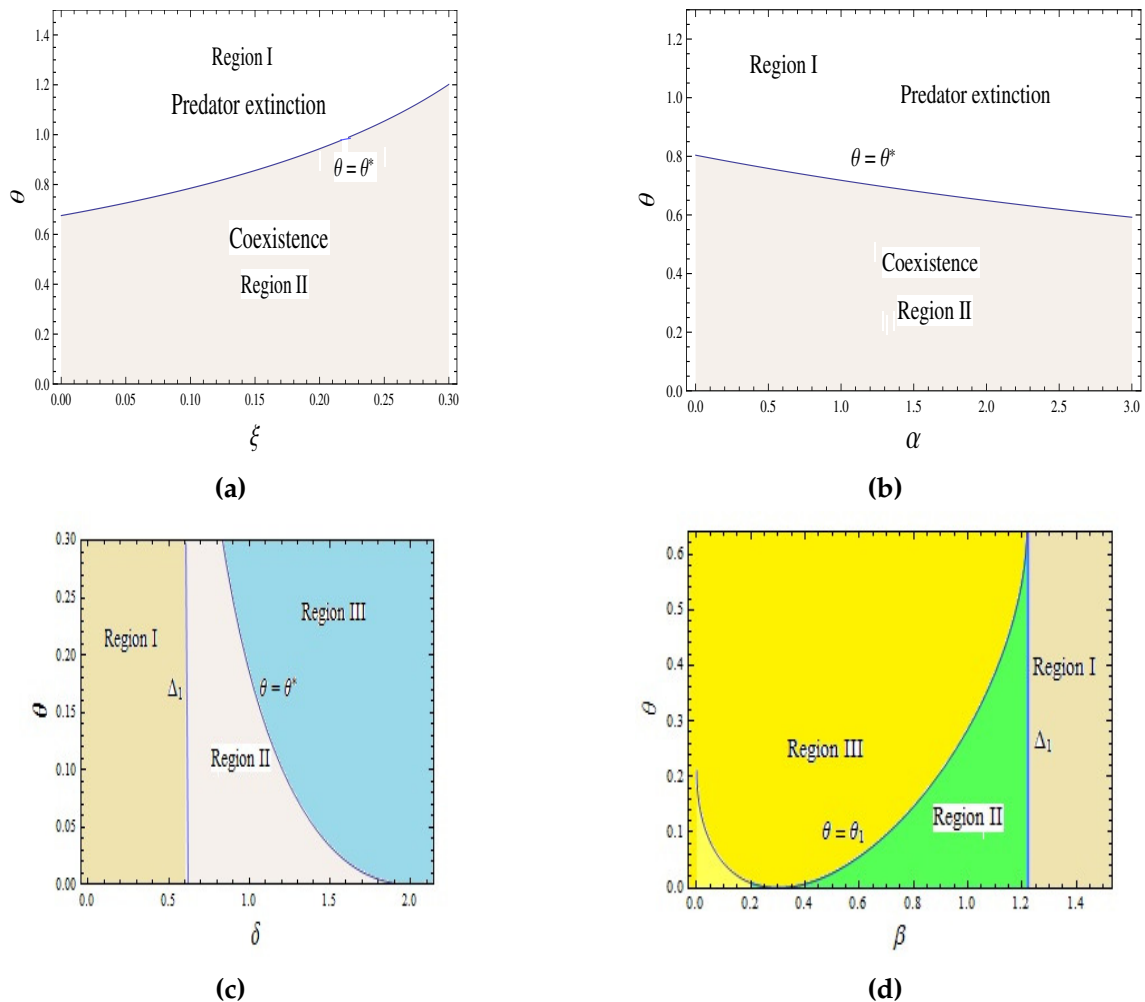


Figure 7. (a) – (b) In region I, predator extinction will occur, while in region II prey and predator will coexist. (c) In region I, either one interior equilibrium point or two axial equilibrium points will exist, while in the region II, two interior and two axial equilibrium points will exist. In region III, only one axial equilibrium point will exist. (d) In region I, one interior and two axial equilibrium points will exist. There are two interiors and two axial equilibrium points on the boundary of regions I and II. In region II, there are two interior and two axial equilibrium points. One interior and two axial equilibrium points will exist on the boundary of II and III regions

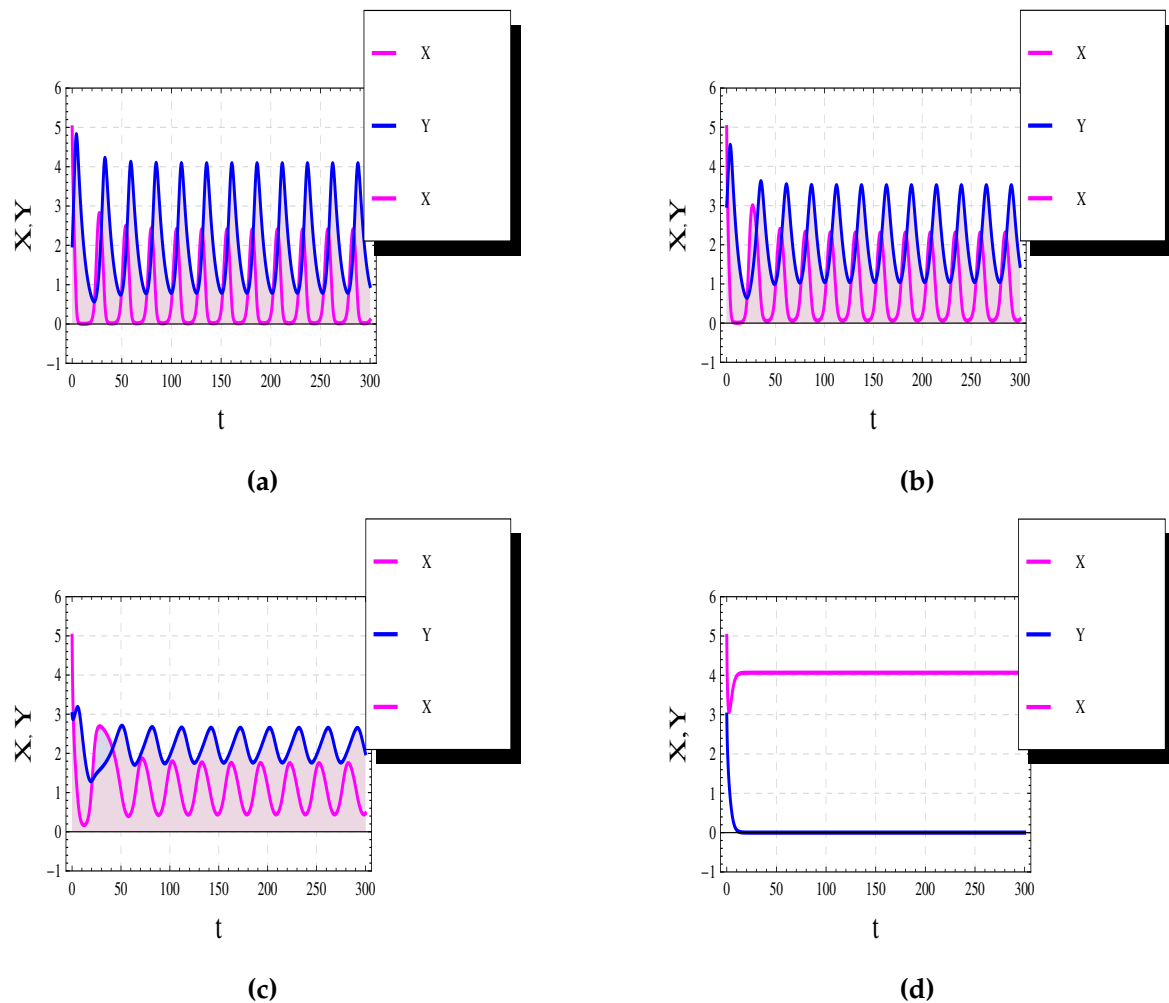


Figure 8. Consider $\alpha = 2.8$, $\beta = 0.9$, $\gamma = 4.06638$, $\delta = 0.3$. Time series solution graph for the system (3) for different values of rate of anti-predator behavior parameter θ (a) $\theta = 0.01$. (b) $\theta = 0.05$. (c) $\theta = 0.1$. (d) $\theta = 0.11$. For small values of θ , the solutions are periodic; however, as θ grows, the period of the solutions diminishes, ultimately leading to the collapse of the periodic solution. Ecologically, both species coexist when θ is small, as θ increases, the predator species will face extinction

8 Conclusion

A qualitative study that considers all factors reveals the model's intriguing, complicated, and diverse dynamics. This manuscript has studied the qualitative analysis of an additional food-provided predator-prey system in the presence of an anti-predator behavior. After developing the model equations and establishing the positivity and boundedness of its solution, we have discussed both theoretically and numerically the local stability of the system around various equilibrium points. It is observed that the system (3) with an anti-predator behavior has at most four equilibrium points, consisting of trivial, predator-free, and interior equilibrium points. It is observed that the trivial equilibrium point will never be stable. Ecologically, it can be stated that the two species cannot go extinct together. Depending on parametric restrictions, the predator-free equilibrium point can be asymptotically stable, or it shows a saddle point. Ecologically, it can be stated that prey species will never go extinct, regardless of the initial population density, but predator species can go extinct under some restrictions. If there are two interior equilibrium points, one will be a saddle point, and the other will be asymptotically stable, unstable, or a stable limit cycle will appear around it, depending on some restrictions. Ecologically, it can be stated that

there is the possibility of coexistence of the species, prey extinction, or oscillation. The system depicts a threatening behavior, bistability, under certain parametric conditions, which indicates the system's sensitivity to initial populations. From an ecological perspective, it may be argued that the long-term survival of a species is contingent upon the size of its original population.

The model displays numerous types of bifurcations, such as saddle-node, Hopf, and BT bifurcations. These bifurcations are an essential part of qualitative analysis and have several ecological consequences. It is observed that the parameters representing the rate of anti-predator behavior of adult prey to predators and the quality and quantity of supplementary food significantly impact the emergence of these bifurcations. If the parameter θ surpasses a specific critical value, model (3) experiences a saddle-node bifurcation, leading to the possibility of zero, one, or two positive interior equilibrium points. As a result, a critical threshold value of θ emerges, below which the coexistence of both populations is possible and beyond which the predator species becomes extinct. Moreover, the manifestation of a limit cycle through Hopf bifurcation has been shown, and the first Lyapunov number can establish the stability of this limit cycle. We have used numerical simulation to indicate that the convergence of a saddle point and a limit cycle might potentially lead to the emergence of homoclinic loops. The system (3) is shown to undergo Bogdanov-Takens bifurcation by selecting the parameters that represent the carrying capacity and the adult prey's anti-predator behavior. Ecologically, it can be stated that certain regions will emerge that exhibit unique qualitative behavior, such as the coexistence of predators and prey in a positive equilibrium state, their coexistence by oscillations, or the eventual extinction of predator species. This study posits that the presence of anti-predator behavior plays a pivotal role in influencing the interactions within a predator-prey system with access to additional food supplies.

This study examined the effects of anti-predator behavior within a two-species predator-prey model. Future research could explore the implications of anti-predator behaviour in ecological systems comprising three or more species, where investigations may assess how anti-predator strategies affect the stability and dynamics of multi-species ecosystems, potentially leading to more complex interactions and behaviours.

Declarations

Use of AI tools

The authors declare that they have not used Artificial Intelligence (AI) tools in the creation of this article.

Data availability statement

There are no external data associated with the manuscript.

Ethical approval (optional)

The authors state that this research complies with ethical standards. This research does not involve either human participants or animals.

Consent for publication

Not applicable

Conflicts of interest

The authors declare that they have no conflict of interest.

Funding

No funding was received for this research.

Author's contributions

M.K.S.: Conceptualization, Methodology, Validation, Writing-Original draft preparation, Software, Supervision, Validation, Formal Analysis. P.P.: Methodology, Writing-Original draft preparation, Data Curation, Software, Writing - Review & Editing. All authors have read and agreed to the published version of the manuscript.

Acknowledgements

Not applicable

References

- [1] Strauss, S.Y. Indirect effects in community ecology: their definition, study and importance. *Trends in Ecology & Evolution*, 6(7), 206-210, (1991). [[CrossRef](#)]
- [2] Savitri, D. Dynamics analysis of anti-predator model on intermediate predator with ratio dependent functional responses. In Proceedings, *The 2nd International Joint Conference on Science and Technology (IJCST)*, pp. 012201-012206, Bali, Indonesia, (2017, September). [[CrossRef](#)]
- [3] Murdoch, W.W., Chesson, J. and Chesson, P.L. Biological control in theory and practice. *The American Naturalist*, 125(3), 344-366, (1985). [[CrossRef](#)]
- [4] Haque, M. and Greenhalgh, D. When a predator avoids infected prey: a model-based theoretical study. *Mathematical Medicine and Biology*, 27(1), 75-94, (2010). [[CrossRef](#)]
- [5] Holt, R.D. and Lawton, J.H. The ecological consequences of shared natural enemies. *Annual Review of Ecology, Evolution, and Systematics*, 25, 495-520, (1994). [[CrossRef](#)]
- [6] Holt, R.D. Predation, apparent competition, and the structure of prey communities. *Theoretical Population Biology*, 12(2), 197-229, (1977). [[CrossRef](#)]
- [7] Sahoo, B. and Poria, S. Disease control in a food chain model supplying alternative food. *Applied Mathematical Modelling*, 37(8), 5653-5663, (2013). [[CrossRef](#)]
- [8] Srinivasu, P.D.N., Prasad, B.S.R.V. and Venkatesulu, M. Biological control through provision of additional food to predators: a theoretical study. *Theoretical Population Biology*, 72(1), 111-120, (2007). [[CrossRef](#)]
- [9] Wade, M.R., Zalucki, M.P., Wratten, S.D. and Robinson, K.A. Conservation biological control of arthropods using artificial food sprays: current status and future challenges. *Biological Control*, 45(2), 185-199, (2008). [[CrossRef](#)]
- [10] Prasad, B.S.R.V., Banerjee, M. and Srinivasu, P.D.N. Dynamics of additional food provided predator-prey system with mutually interfering predators. *Mathematical Biosciences*, 246(1), 176-190, (2013). [[CrossRef](#)]
- [11] Sahoo, B. and Poria, S. Effects of supplying alternative food in a predator-prey model with harvesting. *Applied Mathematics and Computation*, 234, 150-166, (2014). [[CrossRef](#)]
- [12] Chakraborty, K. and Das, S.S. Biological conservation of a prey-predator system incorporating constant prey refuge through provision of alternative food to predators: a theoretical study. *Acta Biotheoretica*, 62, 183-205, (2014). [[CrossRef](#)]
- [13] Sen, M., Srinivasu, P.D.N. and Banerjee, M. Global dynamics of an additional food provided

- predator-prey system with constant harvest in predators. *Applied Mathematics and Computation*, 250, 193-211, (2015). [[CrossRef](#)]
- [14] Shome, P., Maiti, A. and Poria, S. Effects of intraspecific competition of prey in the dynamics of a food chain model. *Modeling Earth Systems and Environment*, 2, 1-11, (2016). [[CrossRef](#)]
- [15] Ghosh, J., Sahoo, B. and Poria, S. Prey-predator dynamics with prey refuge providing additional food to predator. *Chaos, Solitons & Fractals*, 96, 110-119, (2017). [[CrossRef](#)]
- [16] Singh, M.K. and Bhadauria, B.S. Qualitative analysis of an additional food provided predator-prey model in the presence of Allee effect. *International Journal of Applied and Computational Mathematics*, 3(Suppl 1), 1173-1195, (2017). [[CrossRef](#)]
- [17] Das, A. and Samanta, G.P. A prey-predator model with refuge for prey and additional food for predator in a fluctuating environment. *Physica A: Statistical Mechanics and its Applications*, 538, 122844, (2020). [[CrossRef](#)]
- [18] Thirthar, A.A., Majeed, S.J., Alqudah, M.A., Panja, P. and Abdeljawad, T. Fear effect in a predator-prey model with additional food, prey refuge and harvesting on super predator. *Chaos, Solitons & Fractals*, 159, 112091, (2022). [[CrossRef](#)]
- [19] Debnath, S., Majumdar, P., Sarkar, S. and Ghosh, U. Memory effect on prey-predator dynamics: Exploring the role of fear effect, additional food and anti-predator behaviour of prey. *Journal of Computational Science*, 66, 101929, (2023). [[CrossRef](#)]
- [20] Ananth, V.S. and Vamsi, D.K.K. Time optimal control studies and sensitivity analysis of additional food provided prey-predator systems involving Holling type III functional response based on quality of additional food. *Journal of Biological Systems*, 31(01), 271-308, (2023). [[CrossRef](#)]
- [21] Das, B.K., Sahoo, D. and Samanta, G. Fear and its carry-over effects in a delay-induced predator-prey model with additional food to predator. *Filomat*, 37(18), 6059-6088, (2023). [[CrossRef](#)]
- [22] Umaroh, S.Z. and Savitri, D. Dynamic analysis of a prey predator model with Holling-type III functional response and anti-predator behavior. *Jurnal Sains, Teknologi dan Industri*, 21(1), 51-57, (2023). [[CrossRef](#)]
- [23] Berryman, A.A. The origins and evolution of predator-prey theory. *Ecology*, 73(5), 1530-1535, (1992). [[CrossRef](#)]
- [24] Ford, J.K. and Reeves, R.R. Fight or flight: antipredator strategies of baleen whales. *Mammal Review*, 38(1), 50-86, (2008). [[CrossRef](#)]
- [25] Ge, D., Chesters, D., Gomez-Zurita, J., Zhang, L., Yang, X. and Vogler, A.P. Anti-predator defence drives parallel morphological evolution in flea beetles. *Proceedings of the Royal Society B: Biological Sciences*, 278(1715), 2133-2141, (2011). [[CrossRef](#)]
- [26] Lima, S.L. Nonlethal effects in the ecology of predator-prey interactions. *Bioscience*, 48(1), 25-34, (1998). [[CrossRef](#)]
- [27] Matassa, C.M., Donelan, S.C., Luttbeg, B. and Trussell, G.C. Resource levels and prey state influence antipredator behavior and the strength of nonconsumptive predator effects. *Oikos*, 125(10), 1478-1488, (2016). [[CrossRef](#)]
- [28] Zanette, L.Y., White, A.F., Allen, M.C. and Clinchy, M. Perceived predation risk reduces the number of offspring songbirds produce per year. *Science*, 334(6061), 1398-1401, (2011). [[CrossRef](#)]

- [29] Panja, P., Mondal, S.K. and Chattopadyay, J. Dynamical effects of anti-predator behavior of adult prey in a predator-prey model with ratio-dependent functional response. *Asian Journal of Mathematics and Physics*, 1(1), 19-32, (2017).
- [30] Khater, M., Murariu, D. and Gras, R. Predation risk tradeoffs in prey: effects on energy and behaviour. *Theoretical Ecology*, 9, 251-268, (2016). [[CrossRef](#)]
- [31] Samanta, S., Mandal, A.K., Kundu, K. and Chattopadhyay, J. Control of disease in prey population by supplying alternative food to predator. *Journal of Biological Systems*, 22(04), 677-690, (2014). [[CrossRef](#)]
- [32] Tang, B. and Xiao, Y. Bifurcation analysis of a predator-prey model with anti-predator behaviour. *Chaos, Solitons & Fractals*, 70, 58-68, (2015). [[CrossRef](#)]
- [33] Mortoja, S.G., Panja, P. and Mondal, S.K. Dynamics of a predator-prey model with stage-structure on both species and anti-predator behavior. *Informatics in Medicine Unlocked*, 10, 50-57, (2018). [[CrossRef](#)]
- [34] Prasad, K.D. and Prasad, B.S.R.V. Qualitative analysis of additional food provided predator-prey system with anti-predator behaviour in prey. *Nonlinear Dynamics*, 96, 1765-1793, (2019). [[CrossRef](#)]
- [35] Sahoo, B., Das, B. and Samanta, S. Dynamics of harvested-predator-prey model: role of alternative resources. *Modeling Earth Systems and Environment*, 2, 140, (2016). [[CrossRef](#)]
- [36] Chen, J., Huang, J., Ruan, S. and Wang, J. Bifurcations of invariant tori in predator-prey models with seasonal prey harvesting. *SIAM Journal on Applied Mathematics*, 73(5), 1876-1905, (2013). [[CrossRef](#)]
- [37] Huang, J., Gong, Y. and Chen, J. Multiple bifurcations in a predator-prey system of Holling and Leslie type with constant-yield prey harvesting. *International Journal of Bifurcation and Chaos*, 23(10), 1350164, (2013). [[CrossRef](#)]
- [38] Perko, L. *Differential Equations and Dynamical Systems* (Vol. 7). Springer: New York, (2001).

Mathematical Modelling and Numerical Simulation with Applications (MMNSA)
(<https://dergipark.org.tr/en/pub/mmnsa>)



Copyright: © 2025 by the authors. This work is licensed under a Creative Commons Attribution 4.0 (CC BY) International License. The authors retain ownership of the copyright for their article, but they allow anyone to download, reuse, reprint, modify, distribute, and/or copy articles in MMNSA, so long as the original authors and source are credited. To see the complete license contents, please visit (<http://creativecommons.org/licenses/by/4.0/>).

How to cite this article: Singh, M.K. & Poonam, P. (2025). Bifurcation analysis of an additional food-provided predator-prey system with anti-predator behavior. *Mathematical Modelling and Numerical Simulation with Applications*, 5(1), 38-64. <https://doi.org/10.53391/mmnsa.1496827>